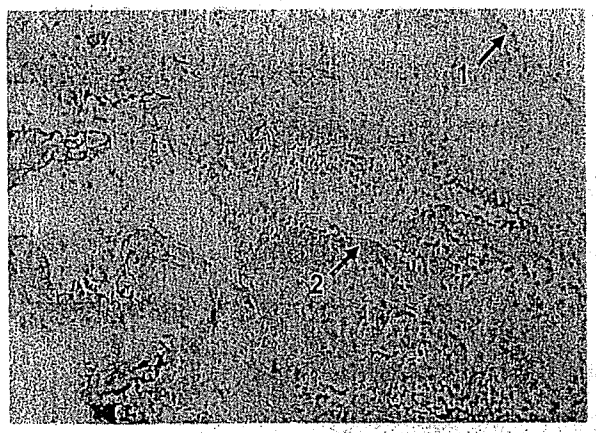

Fig 2. Photomicrograph (hematoxylin–eosin staining, ×400) of the cyst wall showing the large cyst lining of the squamous epithelium (arrow 1), and within the fibrous wall of the large cyst, a smaller cyst lined by similar squamous epithelium (arrow 2) is shown.

atrioventricular node became a defect after the wall of the cyst was completely resected. It was closed directly with 6-0 monofilament sutures. Complete atrioventricular block persisted after surgery and a permanent pacemaker was inserted 11 days later.

Histopathological examination revealed that the cyst wall was composed of fibrous connective tissue covered by a layer of squamous epithelium with partial cornification.[4] Within the fibrous tissue were smaller cysts lined by a similar epithelium (Fig 2). Immunohistochemical staining showed that the cells of the cyst expressed carcinoembryonic antigen and epithelial membrane antigen, suggesting that they were of endodermal origin.

The patient's recovery was uneventful and her symptoms completely disappeared. A 5-year follow-up has revealed no evidence of recurrence of the tumor.

Discussion

Cystic tumor of the atrioventricular nodal region was first described in 1911.[5] It is a rare primary cardiac tumor located in the region of the atrioventricular node. According to previous reports,[1–3,6] it can cause variable degrees of heart blockage, which gradually evolve to complete heart blockage. Moreover, ventricular tachycardia or fibrillation sometimes occurs in patients with this tumor.[2,3,6] Tumor size varies from 0.5 mm to 30 mm, and there is no relationship between size and the occurrence of lethal arrhythmia. It is thus important to consider the possibility of cystic tumor of the atrioventricular nodal region in patients with electrocardiographic evidence of heart block limited to the atrioventricular node (ie, with a narrow QRS), particularly in women.[2]

This tumor is thought to be of embryologic origin and not a true neoplasm because of its benign histological appearance and invariable location in the atrioventricular area. The atrioventricular nodal region is an area of embryologic fusion, suggesting that either mesothelium or nearby foregut inclusion could be incorporated in it. The immunohistochemical findings in this case, which corresponded with those of other recently reported cases,[1,6–9] suggested that the tumor was an endodermal and not mesothelial remnant.

The cause of lethal arrhythmia in patients with cystic tumor of the atrioventricular nodal region is uncertain. Complete heart blockage or associated dysfunction of the sinus node might cause excessive distention of the ventricle and lead to ventricular fibrillation. However, this hypothesis does not explain why lethal arrhythmia often occurs just after the beginning of electronic pacing.[10]

The first case of successful resection of this tumor was reported in 1992 by Balasundaram et al.[7] In their case, the atrioventricular node tumor was only 0.5 mm in diameter and was an unexpected finding associated with an ostium secundum atrial septal defect. Paniagua et al reported the first case in which this type of tumor was detected preoperatively by echocardiography and MRI.[8] Kaminishi et al recently reported the successful prevention of heart blockage by leaving the cyst wall attached to the base of the IAS.[9] There was no sign of residual mass or recurrence 12 months after surgery. It is controversial whether the cyst should be resected completely from the base of the IAS. However, because one complication of this tumor is sudden death as a result of ventricular tachycardia or ventricular fibrillation,[2,3,6] we believe that complete resection is essential, even if subsequent pacemaker implant is required.

References

1. Bruke AP, Anderson PG, Virmani R, James TN, Herrera GA, Ceballos R. Tumor of the atrioventricular nodal region. *Arch Pathol Lab Med* 1990; **114:** 1057–1062.
2. Nishida K, Kamijima G, Nagayama T. Mesothelioma of the atrioventricular node. *Br Heart J* 1985; **53:** 468–470.
3. Travers H. Congenital polycystic tumor of the atrioventricular node: Possible familial occurrence and critical review of reported cases with special emphasis on histogenesis. *Hum Pathol* 1982; **13:** 25–35.
4. Nojima Y, Ishibashi-Ueda H, Yamagishi M. Cystic tumor of the atrioventricular node. *Heart* 2003; **89:** 122.
5. Armstrong H, Monckeberg JG. Herzblock, bedingt druch primaren Herztumor, bei einem 5 jahrigen Kinde. *Dtsch Arch Klin Med* 1911; **102:** 144–166.
6. Monma N, Sotodate R, Tashiro A, Segawa I. Origin of so-called mesothelioma of the atrioventricular node. *Arch Pathol Lab Med* 1991; **115:** 1026–1029.
7. Balasundaram S, Halees SA, Duran C. Mesothelioma of the atrioventricular node: First successful follow-up after excision. *Eur Heart J* 1992; **13:** 718–719.
8. Paniagua JR, Sadaba JR, Davidson LA, Munsch CM. Cystic tumor of the atrioventricular nodal region: Report of a case successfully treated with surgery. *Heart* 2000; **83:** E6.
9. Kaminishi Y, Watanabe Y, Nakata H, Shimokama T, Jikuya T. Cystic tumor of the atrioventricular nodal region. *Jpn J Thorac Cardiovasc Surg* 2002; **50:** 37–39.
10. James TN, Galakhov I. Fatal electrical instability of the heart associated with benign congenital polycystic tumor of the atrioventricular node. *Circulation* 1977; **56:** 667–678.

Circ J 2005; **69**: 1180–1185

Elevation of Plasma Matrix Metalloproteinase-9 in the Culprit Coronary Artery in Patients With Acute Myocardial Infarction

— Clinical Evidence From Distal Protection —

Shuichiro Higo, MD; Masaaki Uematsu, MD; Masakazu Yamagishi, MD*; Hatsue Ishibashi-Ueda, MD**; Masaki Awata, MD; Takakazu Morozumi, MD; Tomoki Ohara, MD; Shinsuke Nanto, MD; Seiki Nagata, MD

Background Although the elevation of circulating plasma matrix metalloproteinase (MMP)-9 levels in patients with acute myocardial infarction (AMI) has been documented, the origin of MMP-9 remains unclear.
Methods and Results Plasma MMP-9 levels in both the peripheral circulation and coronary arteries were measured in patients with AMI (n=23) and with stable angina pectoris (SAP, n=10) during percutaneous coronary intervention (PCI) with a distal protection device. Blood samples were collected from the femoral artery (FA) and the coronary artery before (Initial) and after (Second) dilation of the culprit lesion. Coronary sinus blood samples were obtained immediately after PCI (n=7). Coronary artery plaque fragments were aspirated in patients with AMI (n=20) and compared with those from patients with SAP who underwent directional atherectomy (n=10). MMP-9 levels in Initial and Second were significantly higher in patients with AMI than in patients with SAP ($p<0.01$). In AMI patients MMP-9 levels were significantly higher in Initial than in the FA ($p<0.05$), and were further increased in Second ($p<0.0001$), whereas those in the coronary sinus were similar to the FA. Immunohistochemistry revealed augmented MMP-9 expression in the coronary artery plaque fragments from AMI patients.
Conclusions MMP-9 is mainly released into the coronary circulation from the coronary artery plaque in patients with AMI. (*Circ J* 2005; **69**: 1180–1185)

Key Words: Acute myocardial infarction; Coronary intervention; Matrix metalloproteinase

Matrix metalloproteinase (MMP), an extracellular matrix degrading enzyme, plays a crucial role in the breakdown of the fibrous cap of plaque and subsequent rupture in the pathogenesis of acute coronary syndrome (ACS)[1,2] The MMP family has been identified in the shoulder regions of human atherosclerotic plaque[3] and is more frequently expressed in the coronary plaque of patients with ACS than with stable angina pectoris (SAP).[4] MMP-9 (92-kDa gelatinase) is associated with atherosclerotic arterial remodeling[5] and is actively synthesized in vulnerable plaque.[6] MMP-9 affects plaque stability in association with various inflammatory cytokines.[7,8] Elevated plasma levels of MMP-9 in the peripheral blood have been shown in patients with ACS[9] and are associated with severe coronary stenosis[10] and cardiovascular mortality.[11] In addition, the plasma MMP-9 level is elevated in the coronary circulation of patients with ACS,[12,13] indicating that the production of MMP-9 may be enhanced in ACS.

MMP release, however, may also occur in the interstitium of ischemic myocardium in the early period after a myocardial infarction (MI),[14] as well as from coronary plaque. The serum MMP concentration is associated with left ventricular remodeling after MI,[15] and in particular, an elevated plasma MMP-9 level is associated with infarct size.[16,17] Hence, whether the main source of increased plasma MMP-9 is the culprit coronary plaque or the infarcted myocardium still remains unclear.

The aim of this study was to determine the major source of plasma MMP-9 in patients with early phase acute MI (AMI) by measuring the plasma levels of MMP-9 in the coronary artery as well as a peripheral artery of patients with AMI and in those with SAP during percutaneous coronary intervention (PCI) using a distal protection device. We also investigated in situ MMP-9 expression in coronary artery plaque aspirated from patients with AMI and compared it with samples obtained by directional coronary atherectomy (DCA) in patients with SAP.

Methods

Patients

We studied 23 consecutive patients with AMI within 24 h from the onset of chest pain (6 women; age range 44–87 years, 64±12 years) and 10 consecutive patients with SAP as the control (5 women; age range 50–71 years, 66±10 years, $p=0.61$ vs AMI). The diagnosis of AMI was determined on the basis of chest pain lasting longer than 30 min with ST-segment elevation >2 mm in at least 2

(Received February 25, 2005; revised manuscript received July 20, 2005; accepted August 3, 2005)
*Kansai Rosai Hospital, Amagasaki, Divisions of *Cardiovascular Medicine and **Pathology, National Cardiovascular Center, Suita, Japan*
Mailing address: Shuichiro Higo, MD, Medicine and Therapeutics, Osaka University Graduate School of Medicine, 2-2, Yamadaoka, Suita 565-0871, Japan. E-mail: higo@medone.med.osaka-u.ac.jp

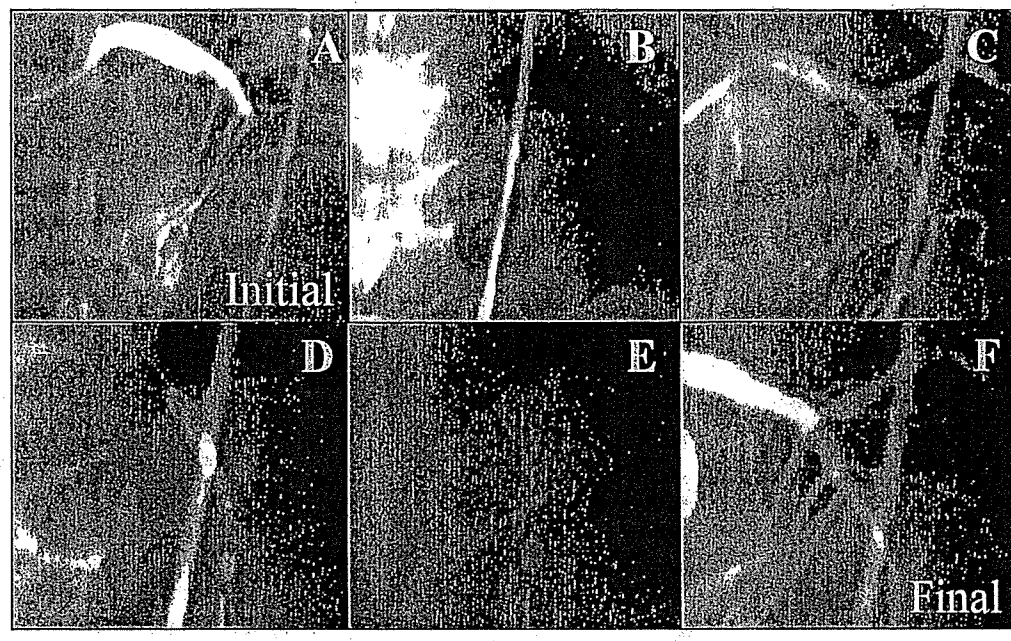

Fig 1. Serial coronary arteriograms showing the intervention procedure. (A) Complete occlusion of the left anterior descending coronary artery. (B) Coronary guidewire crossing the culprit lesion, followed by thrombus aspiration with an aspiration catheter (Initical blood sampling). (C) Coronary arteriogram immediately after the initial aspiration. Thrombolysis In Myocardial Infarction 3 flow grade was obtained in 21 of 23 cases (91%). (D) PercuSurge GuardWire™ also crossing the lesion, parallell with the coronary guidewire. Direct stenting and/or balloon angioplasty was performed under distal protection. (E) Second aspiration (Second blood sampling) to collect material released from the disrupted plaques. (F) Final coronary arteriogram after deflation of the distal occlusion balloon shows restored coronary flow.

contiguous leads of the electrocardiogram, and with more than a 3-fold increase in serum creatine kinase level. Patients with SAP were those who complained of chest pain on exertion with evidence of myocardial ischemia in whom critical coronary stenosis was confirmed by coronary arteriography. All subjects underwent PCI under distal protection with the PercuSurge GuradWire System (Medtronic AVE). Patients with AMI were transferred to the catheterization laboratory and PCI was performed within 1 h of admission. Patients unsuitable for the distal protection procedure because of triple vessel disease, cardiogenic shock or any other serious conditions were excluded. Patients with renal failure, liver function abnormality, and those with a systemic inflammatory disease were also excluded. Oral antiplatelet therapy (200 mg/day aspirin and 200 mg/day ticlopidine) was begun after PCI unless contraindicated. The Ethics Committee of the Kansai Rosai Hospital approved the study protocol and all patients gave written informed consent before cardiac catheterization.

Distal Protection Device

A balloon-type temporary occlusion and aspiration system for the coronary artery (PercuSurge GuardWire™ System) was used for distal protection during PCI and blood sampling from the coronary artery. Detailed specifications of the system are described elsewhere![18,19] In brief, it consists of a guidewire with a distal occlusion balloon (GuardWire Plus), an aspiration catheter (Export), MicroSeal Adapter and EZ Flator inflating system. Guard Wire Plus comprises a 0.014-inch nitinol hypotube with an inflatable internal lumen, which is connected to the occlusion balloon (3–6 mm in diameter) at the end. Export Aspiration catheter is a 0.071-inch monorail-type aspiration catheter incorporating a 0.040-inch lumen that requires an 8Fr guide catheter. GuardWire Plus is connected to the MicroSeal Adapter and EZ Flator, which adjust the size of the distal occlusion balloon under low pressures less than 1 atm. This distal protection and aspiration system enabled us to take selective blood samples from the PCI site in the coronary artery.

PCI With Distal Protection Prior to PCI each patient was given 10,000 units and additional heparin was administrated during the procedure to maintain the activated clotting time >250 s. First, the culprit lesion was crossed with a 0.014-inch angioplasty guidewire and then the Export Aspiration catheter was advanced to the culprit lesion for extensive aspiration while advancing and retracting the catheter (initial aspiration: Initial). The SAP patients underwent the same procedure, although none had a total occlusive lesion. Next, the PercuSurge GuardWire was advanced beyond the lesion, parallel with the guidewire and balloon angioplasty or direct stenting was performed while the distal occlusion balloon inflated the lumen 0.5–1.0 mm larger than the diameter of the reference vessel. After satisfactory dilation had been achieved, the Export Aspiration catheter was again inserted just proximal to the distal occlusion balloon, and aspiration was repeated (second aspiration: Second). Finally, the distal balloon was deflated and antegrade coronary flow was restored. The procedure was completed by ascertaining Thrombolysis In Myocardial Infarction (TIMI) 3 coronary blood flow without any interventional complications. Additional angioplasty was performed if necessary. Patients with AMI and those with SAP underwent the similar procedure. A representative series of coronary arteriograms during the procedure are shown in Fig 1.

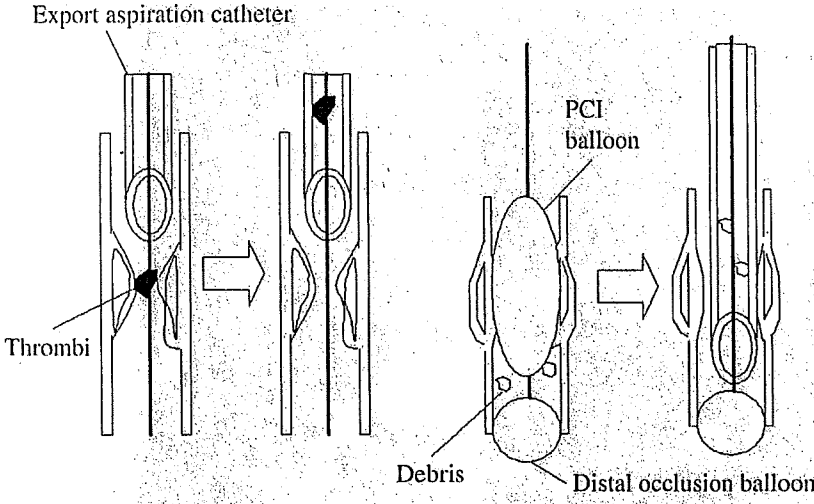

Fig 2. Schematic illustrations of the Initial (Left) and Second (Right) blood samplings. Coronary blood was initially aspirated with an Export aspiration catheter in all patients, regardless of the presence or absence of occlusive thrombi (Left). Immediately after balloon dilatation of the culprit lesion under distal protection, coronary blood, including plaque debris, was aspirated again (Right). PCI, percutaneous coronary intervention.

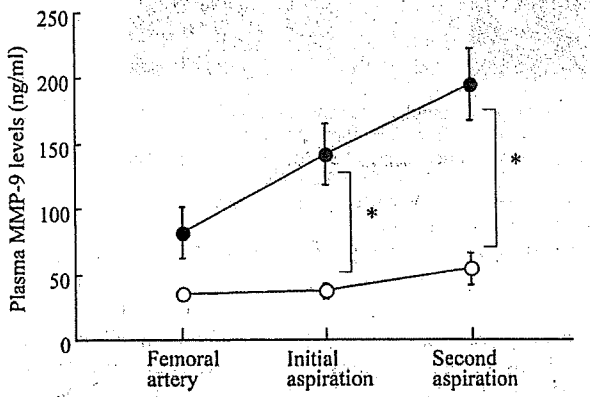

Fig 3. Comparison of plasma matrix metalloproteinase (MMP)-9 levels in patients with acute myocardial infarction (AMI) and those with stable angina pectoris (SAP) during percutaneous coronary intervention. MMP-9 levels in Initial and Second are significantly elevated in patients with AMI compared with those in patients with SAP. Data are expressed as mean±SE. (Solid circles) Patients with AMI; (Open circles) patients with SAP. *p<0.01.

MMP-9 Measurement

Blood samples were obtained from the femoral artery (FA) at the beginning of PCI and during the first and second aspirations from the coronary artery (Fig 2). Blood from the coronary artery was directly collected into the collection bottle without filtration. In 7 AMI patients, a thermodilution catheter was inserted via the internal jugular vein after the PCI, and samples from the coronary sinus (CS) were collected simultaneously using a 5F Multipurpose catheter (Goodman). The blood was immediately mixed with sodium EDTA, centrifuged at 3,000 rpm for 5 min, separated and stored at −80°C. Plasma levels of MMP-9 were measured by one-step sandwich enzyme immunoassay using 2 monoclonal antibodies (Daiichi Fine Chemical)[20]

Immunohistochemistry

Subgroups of AMI and SAP patients were selected for immunohistochemistry. The AMI group comprised 20 patients (3 women; age range 44–82 years) from whom coronary plaque was successfully obtained during the emergency PCI. These patients underwent aggressive intracoronary aspiration using an aspiration catheter (Resque™ Thrombectomy System, Boston Scientific), and thrombi that included fragments of the coronary plaque were obtained. The SAP group comprised 10 patients (4 women; age range 55–65 years) from whom coronary plaque samples were while they underwent elective DCA.

MMP-9 Staining Specimens were placed in tissue fixative (Histochoice, Hedwin, Baltimore, MD, USA). After overnight fixation, they were embedded in paraffin and sectioned at 4• m intervals. Tissue sections were deparaffinized with xylene followed by immersion in a graded alcohol series. They were washed 3 times for 5 min each in phosphate-buffered saline (PBS) and blocked with bovine serum albumin for 60 min. Specimens were then incubated with primary antibodies against MMP-9 (Fuji Chemical, Tokyo, Japan) overnight at 4°C. After being washed in PBS, they were incubated with biotinylated rabbit anti-mouse IgG for 60 min at room temperature. Specimens were then washed with PBS, stained with horseradish peroxidase-conjugated streptavidin, and finally incubated with substrate solution for 1–15 min. The tissue sections were also stained with hematoxylin-eosin. MMP expression was semiquantitatively graded as 0 if there was no staining in any visual field, 1 if <25% cells were stained, 2 if <50% cells were stained and 3 if >50% cells and extracellular matrix were positive for staining. Grading of immunohistochemistry staining was performed by pathologists unaware of the patients' backgrounds.

Statistical Analysis

Data are expressed as mean±SEM, unless otherwise indicated. One-way factorial analysis of variance (ANOVA) followed by Sheffe's post hoc test was used for intergroup comparisons. Two-factor ANOVA or unpaired t-test was applied to evaluate the difference between the groups. Mann-Whitney's U test was used to compare the staining grade. A probability value of less than 0.05 was considered statistically significant.

Results

Plasma MMP-9 Measurement

AMI vs SAP Plasma MMP-9 levels were elevated at any sampling point in patients with AMI, whereas they fell within the normal range of 38±13 ng/ml[20] in patients with

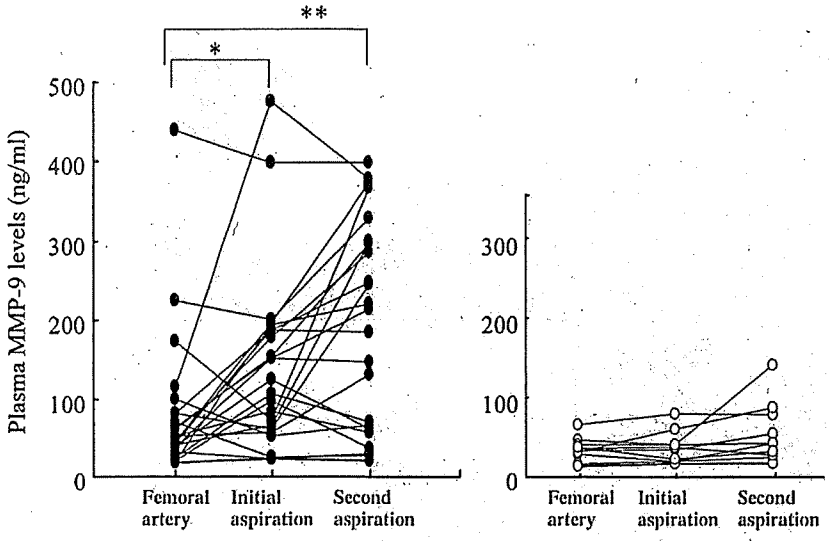

Fig 4. Individual values of plasma matrix metalloproteinase (MMP)-9. In patients with acute myocardial infarction (AMI), MMP-9 levels in Initial were significantly higher than those in the femoral artery, and further increased in Second (Left panel). In patients with stable angina pectoris (SAP), MMP-9 levels remained within the normal range throughout the percutaneous coronary intervention procedure (Right panel). (Solid circles) Patients with AMI; (Open circles) patients with SAP. *p<0.05, **p<0.0001.

SAP (Fig 3). MMP-9 levels in the coronary artery, both Initial and Second, were significantly higher in patients with AMI than in those with SAP (Initial, 141.6±23.3 ng/ml vs 37.2±6.3 ng/ml, p<0.01; Second, 194.9±27.3 ng/ml vs 54.2±12.0 ng/ml, p<0.01) although there was no statistical difference regarding the MMP levels in the systemic circulation, in FA, between patients with AMI and those with SAP.

Variation of MMP-9 Level Among the Sampling Points

MMP-9 levels in Initial were significantly higher than those in the FA (141.6±23.3 ng/ml vs 81.9±19.2 ng/ml, p<0.05) in patients with AMI, and they further increased in Second (194.9±27.3 ng/ml, p<0.0001 vs FA) (Fig 4). MMP-9 levels in the FA were also elevated in some patients with AMI and they remained high throughout the PCI procedure in those patients. In contrast, MMP-9 levels remained within the normal range in patients with SAP throughout the PCI procedure (Fig 4). MMP-9 levels in the CS were similar to those in the FA despite the elevation in the coronary artery, particularly in Second (Fig 5).

Immunohistochemistry

Hematoxylin-eosin staining of the plaque samples aspirated from patients with AMI revealed both thrombi and atheromatous tissue, in which many macrophages strongly positive for MMP-9 were present (Fig 6). In contrast, specimens from patients with SAP had MMP-9 negative to moderately positive cells (Fig 6). The cell-associated staining grade for MMP-9 was 0 in 2 samples (10%), 2 in 3 samples (15%), and 3 in 15 samples (75%) in patients with AMI. Compared with 0 in 8 samples (80%), 1 in 1 sample (10%), 2 in 1 sample (10%), and no samples showing grade 3 from patients with SAP. This semiquantitative grading demonstrated that MMP-9 expression was significantly augmented in the specimens from patients with AMI (p<0.0001).

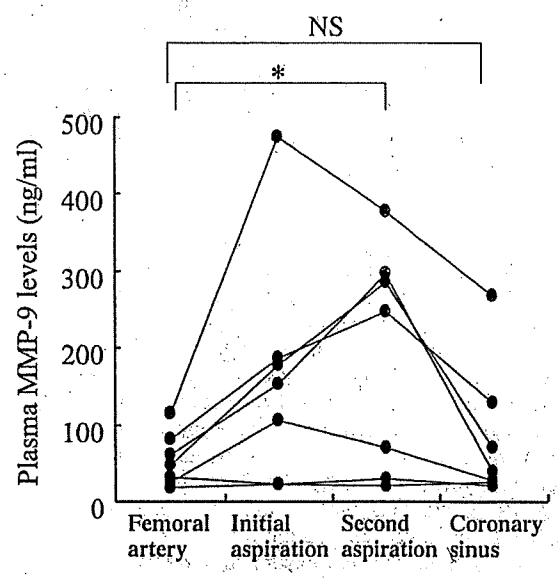

Fig 5. Comparison of matrix metalloproteinase (MMP)-9 levels in the femoral artery, coronary artery and coronary sinus in 7 patients with acute myocardial infarction. MMP-9 levels are elevated in the coronary artery, but not in the coronary sinus, compared with the femoral artery. *p<0.05.

Discussion

The present study demonstrates for the first time that the plasma levels of MMP-9 are significantly higher in the coronary artery than in the systemic circulation (FA and CS) in patients with AMI. Mechanical disruption of the culprit plaque by PCI induces a further elevation of the MMP-9 level in the coronary artery. These elevations were not observed in patients with SAP. In addition, immunohistochemistry revealed augmented MMP-9 expression in the coronary plaque from patients with AMI. Given these findings, the increase in the plasma MMP-9 level in patients with AMI is mainly attributable to the rupture of the culprit plaque in the coronary artery, rather than to the production from necrotic myocardium downstream.

Earlier immunohistochemistry studies on human coronary artery specimens obtained by directional atherectomy revealed localization of MMP-9 in the coronary artery plaque, associated with ischemic heart disease. Larger numbers of MMP-9-positive macrophages were contained within atherectomy specimens from patients with unstable angina pectoris than in those with SAP.[4] MMP-9 was shown to be actively synthesized by macrophages and

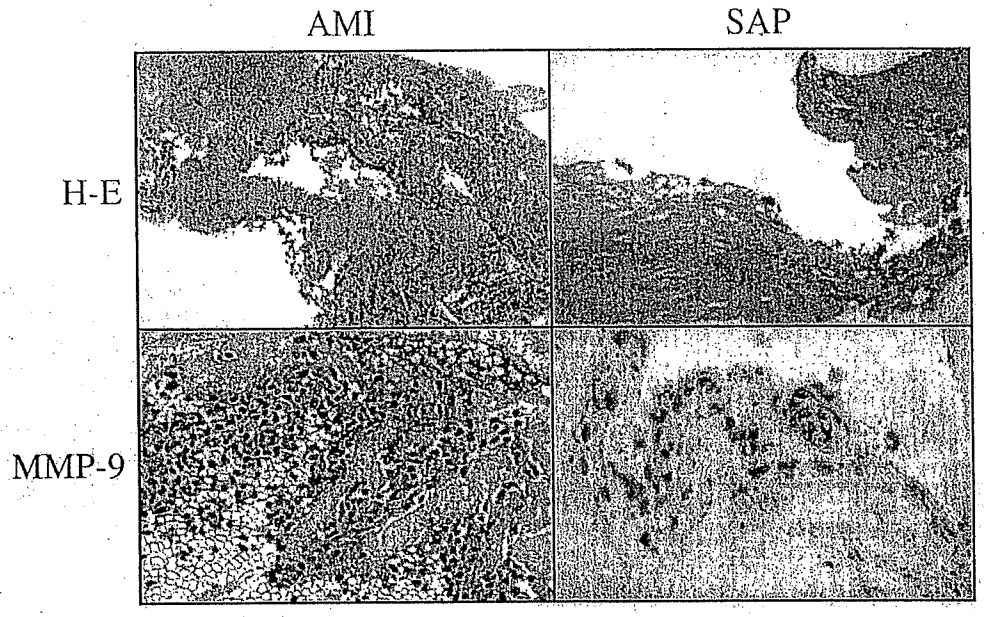

Fig 6. Histology of the aspirated specimen from a case of acute myocardial infarction (AMI) (Left) and the specimen obtained by directional atherectomy in a patient with stable angina pectoris (SAP) (Right). (Upper panels) Hematoxylin-eosin (HE) staining; (Lower panels) immunohistochemistical staining for matrix metalloproteinase (MMP)-9. Left panels demonstrate both thrombotic and atheromatous plaque segments. A number of macrophages are strongly positive for MMP-9 (Lower left). In contrast, MMP-9 was negative to moderately positive in the SAP specimen (Lower right).

smooth muscle cells in the atherosclerotic lesions of the coronary artery in patients with unstable angina pectoris[6] These reports uniformly indicated augmented in vivo MMP-9 localization in the atheromatous plaque and its potential role in plaque vulnerability. Thus, atherosclerotic plaque may be the major source of MMP-9 released into the circulation. However, MMP-9 release and activation were also demonstrated in the ischemic myocardial interstitium in the early post-MI period in animals[14,21] Thus, the necrotic myocardium could also be the predominant source of MMP-9. Previous blood sampling from the CS[12] was unable to exclude the production of MMP by necrotic myocardial tissue. In the present study, however, selective blood sampling using the PercuSurge distal protection device together with CS sampling demonstrated in vivo the elevation of plasma MMP-9 levels in the coronary artery in patients during the acute phase of an AMI. Recently, Funayama et al also reported elevated MMP-9 levels in the human coronary artery[13] but they did not refer to the influence of PCI nor did they simultaneously measure the MMP-9 levels in the CS blood.

Local blood concentration or dilution may affect the measured values, and elevation of circulating plasma MMP-9 levels alone does not directly prove in situ expression in coronary artery plaque. Hence, we immunohistochemically demonstrated augmented expression of MMP-9 and associated inflammatory cells in the coronary artery plaque obtained from patients with AMI. Immunohistochemistry, as well as the blood samples, indicated that culprit plaque and associated inflammatory cells contained large amounts of MMP-9, which would be released into the coronary circulation by mechanical disruption.

Interestingly, patients with AMI who demonstrated TIMI 0 flow in the first coronary arteriogram showed relatively higher levels of MMP-9 in the initial aspiration samples than those who demonstrated TIMI 1–3 flow (165.7±30.6 ng/ml vs 86.8±21.0 ng/ml, p=0.12). It is interesting to speculate that MMP-9 content may vary depending on the local thrombus burden. Of note, MMP-9 may induce thrombus formation through degradation of the tissue factor pathway inhibitor, as reported for porcine coronary arteries[22] Further increases in the MMP-9 level in the second aspiration samples taken in our study indicate that mechanical disruption of the culprit plaque in AMI causes MMP-9 release into the coronary circulation, which may also further aggravate thrombus formation during coronary intervention.

Recently, plasma MMP-9 has been identified as a novel indicator of cardiovascular mortality in patients with coronary artery disease[11] Together with the data from our study, this suggests that plasma MMP-9 may not only be a risk marker, but also an indicator of atherosclerotic plaque vulnerability in patients with ischemic heart disease. Nonetheless, our data failed to show a difference between the AMI and SAP groups in MMP-9 levels in the FA, suggesting that care should be taken to interpret systemic biomarkers for coronary artery disease.

Study Limitations

The study population was relatively small, although the elevation of the MMP-9 level reached statistical significance. A larger population including a variety of re-flow conditions would be of interest. Because all blood samples were obtained only during a PCI procedure performed in the acute phase, these results can not refer to the subsequent clinical course of AMI patients. In the immunohistochemistry study, aspirated specimens were compared with DCA samples. It would be desirable to use the same DCA method to obtain tissue specimens from patients with AMI, but as this is seldom performed in the clinical setting of AMI, we used fragmented coronary artery plaque obtained by the aspiration technique.

Conclusion

Analysis of blood samples from a peripheral artery, the coronary artery and the CS during PCI, together with immunohistochemical staining of plaque, indicate that MMP-9 is mainly released into the coronary circulation, not from the myocardium, but from the culprit coronary artery plaque in patients with AMI.

Acknowledgments

We gratefully acknowledge the expert assistance of Drs Toshinari Onishi, Osamu Iida and Noriaki Ito in performing cardiac catheterization.

References

1. Libby P. Molecular bases of the acute coronary syndromes. *Circulation* 1995; **91:** 2844–2850.
2. Shah PK, Falk E, Badimon JJ, Fernandez-Ortiz A, Mailhac A, Villareal-Levy G, et al. Human monocyte-derived macrophages induce collagen breakdown in fibrous caps of atherosclerotic plaques: Potential role of matrix-degrading metalloproteinases and implications for plaque rupture. *Circulation* 1995; **92:** 1565–1569.
3. Galis ZS, Sukhova GK, Lark MW, Libby P. Increased expression of matrix metalloproteinases and matrix degrading activity in vulnerable regions of human atherosclerotic plaques. *J Clin Invest* 1994; **94:** 2493–2503.
4. Kaartinen M, van der Wal AC, van der Loos CM, Piek JJ, Koch KT, Becker AE, et al. Mast cell infiltration in acute coronary syndromes: Implications for plaque rupture. *J Am Coll Cardiol* 1998; **32:** 606–612.
5. Pasterkamp G, Schoneveld AH, Hijnen DJ, de Kleijn DP, Teepen H, van der Wal AC, et al. Atherosclerotic arterial remodeling and the localization of macrophages and matrix metalloproteases 1, 2 and 9 in the human coronary artery. *Atherosclerosis* 2000; **150:** 245–253.
6. Brown DL, Hibbs MS, Kearney M, Loushin C, Isner JM. Identification of 92-kD gelatinase in human coronary atherosclerotic lesions: Association of active enzyme synthesis with unstable angina. *Circulation* 1995; **91:** 2125–2131.
7. Saren P, Welgus HG, Kovanen PT. TNF-alpha and IL-1beta selectively induce expression of 92-kDa gelatinase by human macrophages. *J Immunol* 1996; **157:** 4159–4165.
8. Kim SH, Kang YJ, Kim WJ, Woo DK, Lee Y, Kim DI, et al. TWEAK can induce pro-inflammatory cytokines and matrix metalloproteinase-9 in macrophages. *Circ J* 2004; **68:** 396–399.
9. Kai H, Ikeda H, Yasukawa H, Kai M, Seki Y, Kuwahara F, et al. Peripheral blood levels of matrix metalloproteases-2 and -9 are elevated in patients with acute coronary syndromes. *J Am Coll Cardiol* 1998; **32:** 368–372.
10. Kalela A, Koivu TA, Sisto T, Kanervisto J, Hoyhtya M, Sillanaukee P. Serum matrix metalloproteinase-9 concentration in angiographically assessed coronary artery disease. *Scand J Clin Lab Invest* 2002; **62:** 337–342.
11. Blankenberg S, Rupprecht HJ, Poirier O, Bickel C, Smieja M, Hafner G. Plasma concentrations and genetic variation of matrix metalloproteinase 9 and prognosis of patients with cardiovascular disease. *Circulation* 2003; **107:** 1579–1585.
12. Inokubo Y, Hanada H, Ishizaka H, Fukushi T, Kamada T, Okumura K. Plasma levels of matrix metalloproteinase-9 and tissue inhibitor of metalloproteinase-1 are increased in the coronary circulation in patients with acute coronary syndrome. *Am Heart J* 2001; **141:** 211–217.
13. Funayama H, Ishikawa SE, Kubo N, Katayama T, Yasu T, Saito M, et al. Increases in interleukin-6 and matrix metalloproteinase-9 in the infarct-related coronary artery of acute myocardial infarction. *Circ J* 2004; **68:** 451–454.
14. Etoh T, Joffs C, Deschamps AM, Davis J, Dowdy K, Hendrick J, et al. Myocardial and interstitial matrix metalloproteinase activity after acute myocardial infarction in pigs. *Am J Physiol Heart Circ Physiol* 2001; **281:** 987–994.
15. Soejima H, Ogawa H, Sakamoto T, Miyamoto S, Kajiwara I, Kojima S, et al. Increased serum matrix metalloproteinase-1 concentration predicts advanced left ventricular remodeling in patients with acute myocardial infarction. *Circ J* 2003; **67:** 301–304.
16. Kaden JJ, Dempfle CE, Sueselbeck T, Brueckmann M, Poerner TC, Haghi D, et al. Time-dependent changes in the plasma concentration of matrix metalloproteinase 9 after acute myocardial infarction. *Cardiology* 2003; **99:** 140–144.
17. Sundström J, Evans JC, Benjamin EJ, Levy D, Larson MG, Sawyer DB, et al. Relations of plasma matrix metalloproteinase-9 to clinical cardiovascular risk factors and echocardiographic left ventricular measures: The Framingham Heart Study. *Circulation* 2004; **109:** 2850–2856.
18. Carlino M, De Gregorio J, Di Mario C, Anzuini A, Airoldi F, Albiero R, et al. Prevention of distal embolization during saphenous vein graft lesion angioplasty: Experience with a new temporary occlusion and aspiration system. *Circulation* 1999; **99:** 3221–3223.
19. Baim DS, Wahr D, George B, Leon MB, Greenberg J, Cutlip DE, et al. Randomized trial of a distal embolic protection device during percutaneous intervention of saphenous vein aorto-coronary bypass grafts. *Circulation* 2002; **105:** 1285–1290.
20. Fujimoto N, Hosokawa N, Iwata K, Shinya T, Okada Y, Hayakawa T. A one-step sandwich enzyme immunoassay for inactive precursor and complexed forms of human matrix metalloproteinase 9 (92 kDa gelatinase/type IV collagenase, gelatinase B) using monoclonal antibodies. *Clin Chim Acta* 1994; **231:** 79–88.
21. Cleutjens JP, Kandala JC, Guarda E, Guntaka RV, Weber KT. Regulation of collagen degradation in the rat myocardium after infarction. *J Mol Cell Cardiol* 1995; **27:** 1281–1292.
22. Morishige K, Shimokawa H, Matsumoto Y, Eto Y, Uwatoku T, Abe K, et al. Overexpression of matrix metalloproteinase-9 promotes intravascular thrombus formation in porcine coronary arteries in vivo. *Cardiovasc Res* 2003; **57:** 572–585.

Transplantation of Mesenchymal Stem Cells Improves Cardiac Function in a Rat Model of Dilated Cardiomyopathy

Noritoshi Nagaya, MD; Kenji Kangawa, PhD; Takefumi Itoh, MD; Takashi Iwase, MD; Shinsuke Murakami, MD; Yoshinori Miyahara, MD; Takafumi Fujii, MD; Masaaki Uematsu, MD; Hajime Ohgushi, MD; Masakazu Yamagishi, MD; Takeshi Tokudome, MD; Hidezo Mori, MD; Kunio Miyatake, MD; Soichiro Kitamura, MD

Background—Pluripotent mesenchymal stem cells (MSCs) differentiate into a variety of cells, including cardiomyocytes and vascular endothelial cells. However, little information is available about the therapeutic potency of MSC transplantation in cases of dilated cardiomyopathy (DCM), an important cause of heart failure.

Methods and Results—We investigated whether transplanted MSCs induce myogenesis and angiogenesis and improve cardiac function in a rat model of DCM. MSCs were isolated from bone marrow aspirates of isogenic adult rats and expanded ex vivo. Cultured MSCs secreted large amounts of the angiogenic, antiapoptotic, and mitogenic factors vascular endothelial growth factor, hepatocyte growth factor, adrenomedullin, and insulin-like growth factor-1. Five weeks after immunization, MSCs or vehicle was injected into the myocardium. Some engrafted MSCs were positive for the cardiac markers desmin, cardiac troponin T, and connexin-43, whereas others formed vascular structures and were positive for von Willebrand factor or smooth muscle actin. Compared with vehicle injection, MSC transplantation significantly increased capillary density and decreased the collagen volume fraction in the myocardium, resulting in decreased left ventricular end-diastolic pressure (11±1 versus 16±1 mm Hg, $P<0.05$) and increased left ventricular maximum dP/dt (6767±323 versus 5138±280 mm Hg/s, $P<0.05$).

Conclusions—MSC transplantation improved cardiac function in a rat model of DCM, possibly through induction of myogenesis and angiogenesis, as well as by inhibition of myocardial fibrosis. The beneficial effects of MSCs might be mediated not only by their differentiation into cardiomyocytes and vascular cells but also by their ability to supply large amounts of angiogenic, antiapoptotic, and mitogenic factors. (*Circulation.* **2005;112:1128-1135.**)

Key Words: myocytes ■ angiogenesis ■ heart failure ■ growth substances ■ transplantation

Despite advances in medical and surgical procedures, congestive heart failure remains a leading cause of cardiovascular morbidity and mortality.[1] Idiopathic dilated cardiomyopathy (DCM), a primary myocardial disease of unknown etiology characterized by a loss of cardiomyocytes and an increase in fibroblasts, is an important cause of heart failure.[2] Although myocyte mitosis and the presence of cardiac precursor cells in adult hearts have recently been reported,[3] the death of large numbers of cardiomyocytes results in the development of heart failure. Thus, restoring lost myocardium would be desirable for the treatment of DCM.

Mesenchymal stem cells (MSCs) are pluripotent, adult stem cells residing within the bone marrow microenvironment.[4] In contrast to their hematopoietic counterparts, MSCs are adherent and can be expanded in culture. MSCs can differentiate not only into osteoblasts, chondrocytes, neurons, and skeletal muscle cells but also into vascular endothelial cells[5] and cardiomyocytes.[6,7] In vitro, MSCs can be induced to differentiate into beating cardiomyocytes by 5-azacytidine treatment.[8] In vivo, MSCs directly injected into an infarcted heart have been shown to induce myocardial regeneration and improve cardiac function.[9] In addition, MSC implantation induces therapeutic angiogenesis in a rat model of hindlimb ischemia through vascular endothelial growth factor (VEGF) production by MSCs.[10,11] Myocardial blood flow abnormalities, even in the presence of angiographically normal coronary arteries, have been documented in patients with DCM.[12]

Received August 18, 2004; revision received April 28, 2005; accepted May 10, 2005.

From the Departments of Regenerative Medicine and Tissue Engineering (N.N., T.I., T.I., S.M.), Internal Medicine (N.N., M.Y., K.M.), Biochemistry (K.K., T.T.), and Cardiac Physiology (Y.M., T.F., H.M.), National Cardiovascular Center Research Institute, Osaka; the Cardiovascular Division (M.U.), Kansai Rosai Hospital, Hyogo; the Tissue Engineering Research Center (H.O.), National Institute of Advanced Industrial Science and Technology, Hyogo; and the Department of Cardiovascular Surgery (S.K.), National Cardiovascular Center, Osaka, Japan.

Reprint requests to Noritoshi Nagaya, MD, Department of Regenerative Medicine and Tissue Engineering, National Cardiovascular Center Research Institute, 5-7-1 Fujishirodai, Suita, Osaka 565-8565, Japan. E-mail nnagaya@ri.ncvc.go.jp

Circulation is available at http://www.circulationaha.org

DOI: 10.1161/CIRCULATIONAHA.104.500447

These findings raise the possibility that transplanted MSCs have beneficial effects on myocardial structure and function via myogenesis and angiogenesis. However, little information is available about the therapeutic potential of MSCs for DCM.

A unique model of myocarditis in the rat has been created by immunization with porcine cardiac myosin,[13] which results in severe heart failure characterized by increased cardiac fibrosis and left ventricular (LV) dilation.[14] Thus, the late phase of this model can serve as a model of DCM.

The purpose of this study was to investigate the following topics: (1) whether transplantation of MSCs induces myogenesis and angiogenesis, decreases collagen deposition in the myocardium, and thereby improves cardiac function in a rat model of DCM and (2) whether the beneficial effects of MSCs are mediated by their differentiation into cardiomyocytes and vascular cells and/or by their supplying angiogenic, antiapoptotic, and mitogenic factors.

Methods

Expansion of Bone Marrow MSCs

MSC expansion was performed according to previously described methods.[4] In brief, we humanely killed male Lewis rats and harvested bone marrow by flushing their femoral and tibial cavities with phosphate-buffered saline (PBS). Bone marrow cells were cultured in α-minimal essential medium supplemented with 10% fetal bovine serum and antibiotics. A small number of cells developed visible symmetric colonies by days 5 to 7. Nonadherent hematopoietic cells were removed, and the medium was replaced. The adherent, spindle-shaped MSC population expanded to $>5\times10^7$ cells within ≈4 to 5 passages after the cells were first plated.

Flow Cytometry

Cultured MSCs were analyzed by fluorescence-activated cell sorting (FACS) (FACScan flow cytometer, Becton Dickinson). Cells were incubated with fluorescein isothiocyanate (FITC)–conjugated mouse monoclonal antibodies against rat CD31 (clone TLD-3A12, Becton Dickinson), CD34 (clone ICO-115, Santa Cruz), CD45 (clone OX-1, Becton Dickinson), CD90 (clone OX-7, Becton Dickinson), vimentin (clone V9, Dako), and smooth muscle actin (SMA; clone 1A4, Dako). FITC-conjugated hamster anti-rat CD29 monoclonal antibody (clone Ha2/5, Becton Dickinson) and rabbit anti-rat c-Kit polyclonal antibody (clone C-19, Santa Cruz) were used. Isotype-identical antibodies served as controls.

Model of DCM

Male Lewis rats weighing 220 to 250 g (Japan SLC Inc, Hamamatsu, Japan) were used in this study. These isogenic rats served as donors and recipients of MSCs to simulate autologous implantation. DCM was produced by inducing experimental myocarditis, as described previously.[13,14] In brief, 1 mg (0.1 mL) of porcine heart myosin (Sigma) was mixed with an equal volume of Freund's complete adjuvant (Sigma) and injected into a footpad on days 1 and 7. Five weeks after immunization, these rats served as a model of heart failure due to DCM.

MSC Transplantation

In a preliminary experiment, we performed dose-response studies to obtain the maximal effects of cell transplantation. Because the effect of 10^6 MSCs was modest, we used 5×10^6 MSCs for transplantation. Five weeks after immunization, we injected a total of 5×10^6 MSCs/100 μL PBS, or PBS alone, into the myocardium at 10 points. In brief, the LV was divided into 3 levels (basal, middle, and apical). The basal and middle levels were each subdivided into 4 segments, and the apical level was subdivided into 2 segments. Injection into each segment was performed with a 27-gauge needle. Sham rats received intramyocardial injections of 100 μL PBS. This protocol resulted in the creation of 3 groups: DCM rats given MSCs (MSC-treated DCM group, n=10); DCM rats given PBS (untreated DCM group, n=10); and sham rats given PBS (sham group, n=10). The Animal Care Committee of the National Cardiovascular Center approved this experimental protocol.

Echocardiographic Studies

Echocardiographic studies were performed by an investigator, blinded to treatment allocation, at 5 weeks after immunization (before treatment) and 4 weeks after cell transplantation (after treatment). Two-dimensional, targeted M-mode tracings were obtained at the level of the papillary muscles with an echocardiographic system equipped with a 7.5-MHz transducer (HP Sonos 5500, Hewlett-Packard).[15] LV dimensions were measured according to the American Society for Echocardiology leading-edge method from at least 3 consecutive cardiac cycles. Fractional shortening was calculated as (LVDd−LVDs)/LVDd×100, where LVDd=LV diastolic dimension and LVDs=LV systolic dimension.

Hemodynamic Studies

Hemodynamic studies were performed 4 weeks after cell transplantation. A 1.5F micromanometer-tipped catheter (Millar Instruments) was inserted into the right carotid artery for measurement of mean arterial pressure.[16] Next, the catheter was advanced into the LV for measurement of LV pressure. Hemodynamic variables were measured with a pressure transducer (model P23 ID, Gould) connected to a polygraph. After completion of these measurements, the left and right ventricles were excised and weighed.

Histological Examination

To detect fibrosis in cardiac muscle, the LV myocardium (n=5 from each group) was fixed in 10% formalin, cut transversely, embedded in paraffin, and stained with Masson's trichrome. Transverse sections were randomly obtained from the 3 levels (basal, middle, and apical), and 20 randomly selected fields per section (n=60 per animal) were analyzed. After each field was scanned and computerized with a digital image analyzer (WinRoof, Mitani Co), collagen volume fraction was calculated as the sum of all areas containing connective tissue divided by the total area of the image.[15]

To detect capillaries in the myocardium, samples of harvested muscle (n=5 each) were embedded in OCT compound (Miles Scientific), snap-frozen in LN_2, cut into transverse sections, and stained for alkaline phosphatase by an indoxyltetrazolium method. Transverse sections were randomly obtained from the 3 levels (basal, middle, and apical), and 5 randomly selected fields per section (n=15 per animal) were analyzed. The number of capillaries was counted by light microscopy at a magnification of ×200. The number of capillaries in each field was averaged and expressed as the number of capillary vessels. These morphometric studies were performed by 2 examiners who were blinded to treatment assignment.

Assessment of Cell Differentiation

Suspended MSCs were labeled with fluorescent dyes with use of a PKH26 red fluorescent cell linker kit (Sigma), as reported previously.[17] Fluorescence-labeled MSCs were injected into the myocardium 5 weeks after immunization. Rats (n=5) were humanely killed 4 weeks after cell transplantation. LV samples were embedded in OCT compound, snap-frozen in LN_2, and cut into sections. Immunofluorescence staining was performed with monoclonal mouse anti-cardiac troponin T (Novo), anti-desmin (Dako), anti-connexin-43 (Sigma), polyclonal rabbit anti–von Willebrand factor (Dako), and monoclonal mouse SMA (Dako). FITC-conjugated IgG antibody (BD Pharmingen) was used as a secondary antibody. To perform quantitative analysis of the magnitude of MSC differentiation into cardiomyocytes, heart cells from each rat (n=5) were isolated by incubation in balanced salt solution containing 0.06% collagenase type II (Worthington Biochemical Co), as reported previously.[18] PKH26/troponin T double-positive cells were detected by FACS.

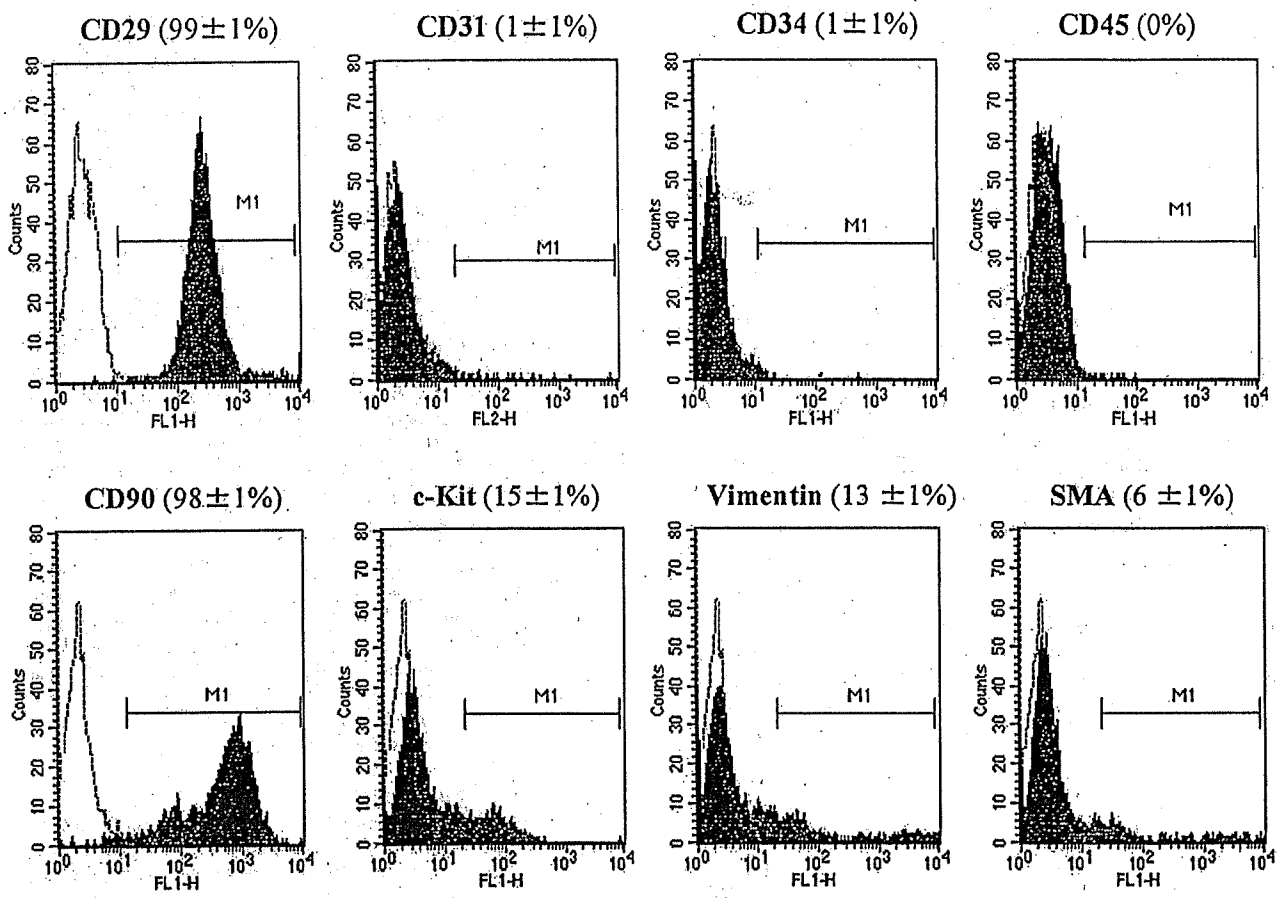

Figure 1. Flow-cytometric analysis of the adherent, spindle-shaped MSC population expanded to 4 to 5 passages. Most of the MSCs expressed CD29 and CD90, whereas they were negative for CD31, CD34, CD45, and SMA. Some of the cells were positive for c-Kit and vimentin.

Western Blot Analysis of Matrix Metalloproteinases

To identify the protein expression of matrix metalloproteinases (MMPs)-2 and -9, Western blotting was performed with rabbit polyclonal antibody raised against MMP-2 (Laboratory vision Co) and MMP-9 (Chemicon Co). The LV obtained from individual rats was used for comparison among the 3 groups (n=5 each). These samples were homogenized on ice in 0.1% Tween 20 homogenization buffer with a protease inhibitor. Then, 40 μg of protein was transferred into sample buffer, loaded on a 7.5% sodium dodecyl sulfate–polyacrylamide gel, and blotted onto a polyvinylidene fluoride membrane (Millipore Co). After being blocked for 120 minutes, the membrane was incubated with primary antibody at a dilution of 1:200. The membrane was incubated with peroxidase labeled with secondary antibody at a dilution of 1:1000. Positive protein bands were visualized with an ECL kit (Amersham) and measured by densitometry. Western blot analysis with a mouse polyclonal antibody raised against β-actin (Santa Cruz) was used as a protein loading control.

Assay for Angiogenic, Antiapoptotic, and Mitogenic Factors

To investigate whether MSCs produce angiogenic and growth factors, we measured VEGF, hepatocyte growth factor (HGF), insulin-like growth factor-1 (IGF-1), and adrenomedullin (AM) levels in conditioned medium 24 hours after medium replacement. VEGF, HGF, and IGF-1 were measured by enzyme immunoassay (VEGF immunoassay, R&D Systems Inc; rat HGF enzyme immunoassay, Institute of Immunology Co, Ltd; and active rat IGF-1 enzyme immunoassay, Diagnostic Systems Laboratories, Inc). AM level was measured with a radioimmunoassay kit (Shionogi Co), as reported previously.[19] The amounts of these products produced by MSCs were compared with those produced by bone marrow–derived mononuclear cells (MNCs) because MNCs have commonly been used for regenerative therapy.[19–21] There was no significant difference in cell viability between MSCs and MNCs 24 hours after seeding (88±5% versus 85±4% by trypan blue solution). In vivo, circulating levels of VEGF, HGF, IGF-1, and AM were measured before and 24 hours after administration of MSCs or vehicle (n=6 from each group).

Statistical Analysis

Numerical values are expressed as mean±SEM unless otherwise indicated. Comparisons of parameters between 2 groups were made with unpaired Student *t* test. Comparisons of parameters among 3 groups were made with a 1-way ANOVA, followed by the Scheffe multiple-comparison test. Comparisons of changes in parameters among the 3 groups were made by a 2-way ANOVA for repeated measures, followed by the Scheffe multiple-comparison test. A value of $P<0.05$ was considered significant.

Results

Characterization of Cultured MSCs

Most cultured MSCs expressed CD29 and CD90 (Figure 1). In contrast, the majority of MSCs were negative for CD31, CD34, CD45, and SMA. Some of the MSCs expressed c-Kit and vimentin.

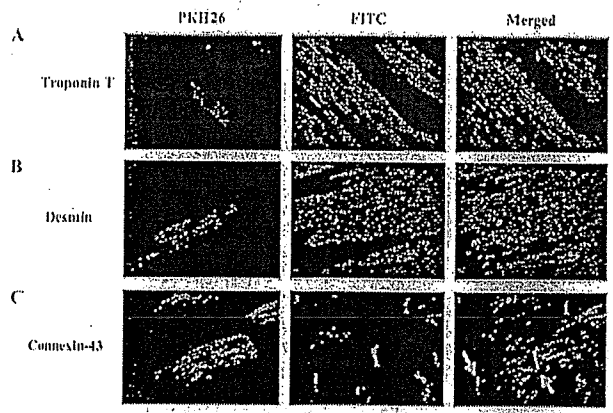

Figure 2. Differentiation of transplanted MSCs into cardiomyocytes. Transplanted MSCs were engrafted in the myocardium and stained for cardiac troponin T (A) and desmin (B). Engrafted MSCs also expressed connexin-43, a gap junction protein, at contact points with native cardiac myocytes (left arrow) and other transplanted cells (right arrow) (C). Magnification ×400.

Myogenesis and Angiogenesis Induced by MSCs

Red fluorescence–labeled MSCs were transplanted into the myocardium 5 weeks after immunization. Four weeks after transplantation, MSCs were engrafted into the myocardium (Figure 2). Immunofluorescence demonstrated that transplanted MSCs were positive for the cardiac markers cardiac troponin T and desmin (Figure 2). Transplanted MSCs also expressed connexin-43, a gap junction protein, at contact points with native cardiac myocytes as well as with MSCs. FACS analysis of isolated heart cells demonstrated that 8±1% of transplanted MSCs were double-positive for PKH26 and troponin T. These results suggest that a small number of transplanted MSCs can differentiate into cardiomyocytes.

Some transplanted MSCs formed vascular structures in the myocardium and were positive for von Willebrand factor (Figure 3A). Other MSCs were positive for SMA and participated in vessel formation as mural cells (Figure 3B). Alkaline phosphatase staining of the ischemic myocardium showed marked augmentation of neovascularization in the MSC-treated DCM group (Figures 4A–4C). Quantitative analysis demonstrated that capillary density was significantly

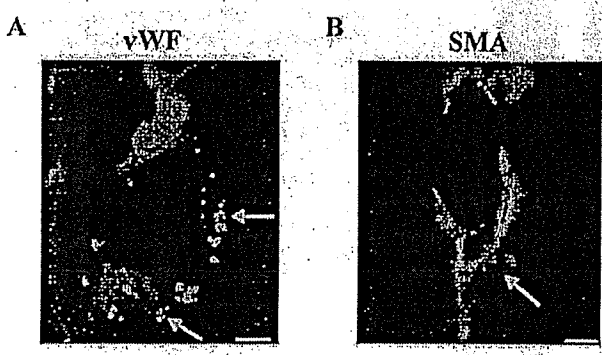

Figure 3. Differentiation of transplanted MSCs into vascular endothelial cells and smooth muscle cells. Some of the transplanted MSCs were positive for von Willebrand factor (vWF, A) and SMA (B) and formed vascular structures (A and B). Scale bars=10 μm.

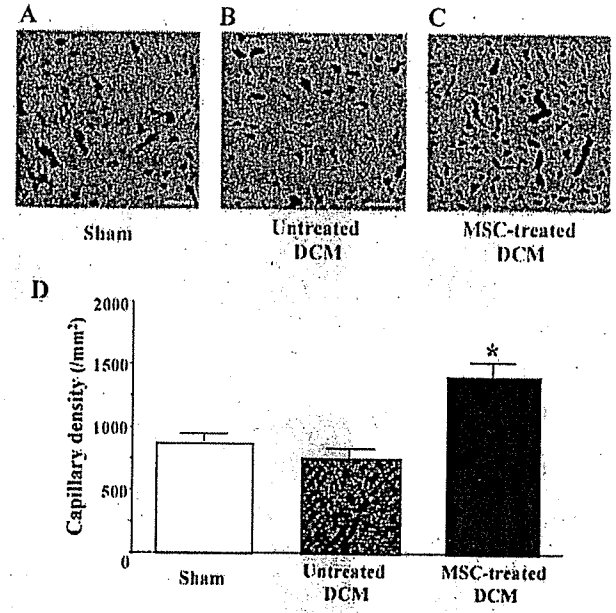

Figure 4. A–C, Representative samples of alkaline phosphatase staining of myocardium. Magnification, ×200. Scale bars=10 μm. D, Quantitative analysis of capillary density in the myocardium. Data are mean±SEM *P<0.05 vs untreated DCM group.

higher in the MSC-treated DCM group than in the untreated DCM group (Figure 4D).

Angiogenic, Antiapoptotic, and Mitogenic Factors Released From MSCs

After 24 hours of culture, MSCs secreted large amounts of angiogenic and antiapoptotic factors, including VEGF, HGF, and AM (Figure 5). Compared with MNCs that have commonly been used for regenerative therapy,[20–22] MSCs secreted 4-fold more VEGF and 5-fold more HGF. Similarly, MSCs secreted 6-fold more AM, an angiogenic and antiapoptotic peptide, compared with MNCs. MSCs also secreted a large amount, 10-fold greater than MNCs, of IGF-1, a growth hormone mediator for myocardial growth (Figure 5). Transplantation of MSCs significantly increased circulating VEGF (45.8±1.6 to 68.5±3.6 pg/mL, P<0.05), HGF (431.8±56.6 to 517.2±67.1 pg/mL, P<0.05), and AM (23.4±0.8 to 41.2±4.8 pg/mL, P<0.05) 24 hours after transplantation, although vehicle injection did not alter these parameters. Serum IGF-1 tended to increase after MSC transplantation (938.1±151.6 to 1063.5±116.9 pg/mL, P=NS), but this increase did not reach statistical significance.

Hemodynamic Effects of MSC Transplantation

Nine weeks after immunization, LV end-diastolic pressure showed a marked elevation in the untreated DCM group; this elevation was significantly attenuated in the MSC-treated DCM group (Figure 6A). LV maximum *dP/dt* was significantly lower in the untreated DCM group than in the sham group (Figure 6B). However, LV maximum *dP/dt* was significantly improved 4 weeks after MSC transplantation. There was no significant difference in heart rate or mean arterial pressure among the 3 groups (the Table). Echocardiographic studies demonstrated LV dysfunction and dilation

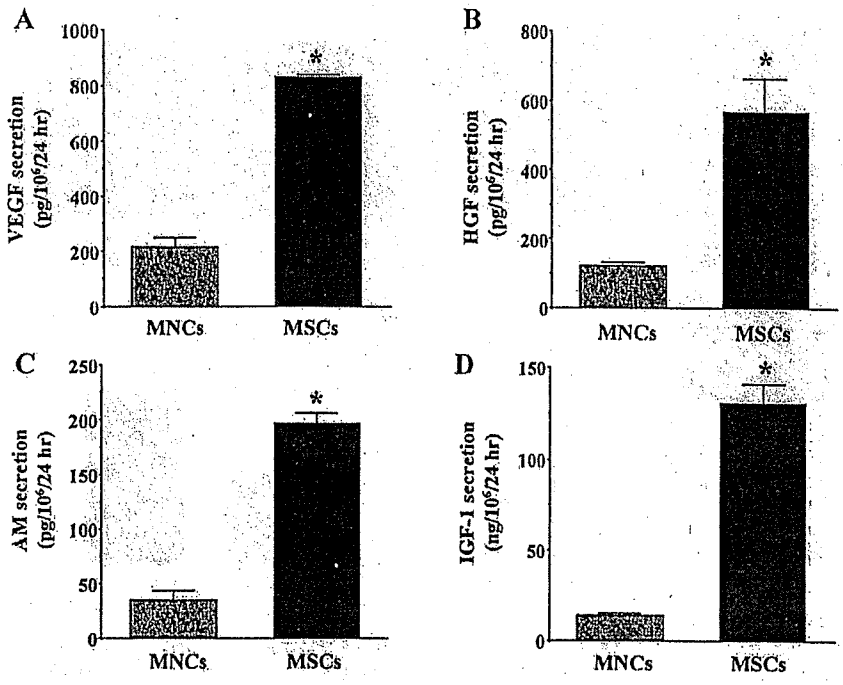

Figure 5. A–D, Angiogenic, antiapoptotic, and mitogenic factors produced by MSCs and bone marrow–derived MNCs). Compared with MNCs, MSCs secreted large amounts of VEGF, HGF, AM, and IGF-1. *$P<0.05$ vs MNCs.

in the untreated DCM group, as indicated by a decrease in percent fractional shortening and an increase in LV diastolic dimension (Figure 6C and 6D). However, MSC transplantation increased percent fractional shortening and inhibited the increase in LV diastolic dimension.

Reduction of Myocardial Fibrosis by MSC Transplantation

Masson's trichrome staining demonstrated modest myocardial fibrosis in the untreated DCM group (Figure 7A). However, MSC transplantation significantly attenuated the development of myocardial fibrosis. Quantitative analysis also demonstrated that the collagen volume fraction in the MSC-treated DCM group was significantly smaller than that in the untreated DCM group (Figure 7B). Western blot analysis showed that myocardial contents of MMP-2 and MMP-9 in the untreated DCM were significantly increased compared with those in the sham group (Figure 7C–E). However, the increases in MMP-2 and MMP-9 levels were attenuated by MSC transplantation, although the change in MMP-9 did not reach statistical significance.

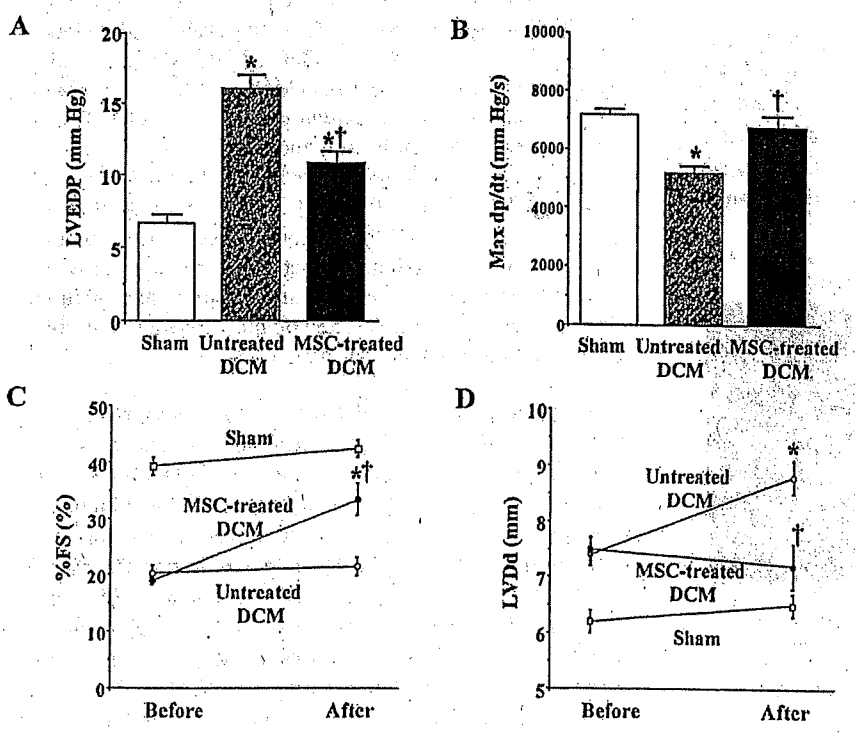

Figure 6. A and B, Effects of MSC transplantation on hemodynamic parameters. LVEDP indicates LV end-diastolic pressure; Max *dP/dt*, LV maximum *dP/dt*. Data are mean±SEM. *$P<0.05$ vs sham group; †$P<0.05$ vs untreated DCM group. C and D, Changes in echocardiographic parameters induced by MSC transplantation. %FS indicates LV fractional shortening. Data are mean±SEM *$P<0.05$ vs before transplantation; †$P<0.05$ vs the time-matched untreated DCM group.

Physiological Profiles of the 3 Experimental Groups

	Sham	Untreated DCM	MSC-Treated DCM
n	10	10	10
Body wt, g	421±8	372±4*	389±5*
LV wt/body wt, g/kg	1.91±0.05	2.18±0.06*	2.05±0.05
RV wt/body wt, g/kg	0.55±0.01	0.68±0.02*	0.60±0.03†
Heart rate, bpm	403±10	432±15	417±12
Mean arterial pressure, mm Hg	134±2	123±3	132±5

wt indicates weight; RV, right ventricle. Sham-operated rats were given vehicle only. The untreated DCM group included DCM rats treated with vehicle. The MSC-treated DCM group included DCM rats treated with MSCs. Data are mean±SEM.

*P<0.05 vs sham group; †P<0.05 vs untreated DCM group.

Discussion

In the present study, we have demonstrated the following effects of MSC transplantation in a rat model of DCM: (1) induction of myogenesis and angiogenesis; (2) differentiation of transplanted MSCs into cardiomyocytes, vascular endothelial cells, and smooth muscle cells; (3) secretion of large amounts of VEGF, HGF, AM, and IGF-1; (4) improvement of cardiac function and inhibition of ventricular remodeling; and (5) decrease in collagen volume fraction in the myocardium.

Earlier studies have shown that transplantation of MSCs improves cardiac function in experimental models of ischemic heart disease.[9,23] However, little information is available about the therapeutic potential of MSCs for chronic heart failure due to DCM. Previous studies have shown that porcine cardiac myosin-induced myocarditis progresses to a chronic phase resembling DCM.[13,14] Thus, we used this model 5 weeks after immunization as an example of experimental DCM.

In the present study, transplanted MSCs were engrafted into the myocardium in a rat model of DCM. Four weeks after transplantation, some of the engrafted MSCs were positively stained for cardiac troponin T and desmin. Transplanted MSCs also expressed connexin-43, a gap junction protein, at contact points with native cardiac myocytes as well as with MSCs. These results suggest that MSCs differentiate into cardiomyocytes in the myocardium and form connections with native cardiomyocytes in rats with DCM. Unlike earlier studies that have used a model of myocardial infarction,[7,9,23] we used a rat model of DCM to demonstrate the engraftment and cardiogenic differentiation of MSCs. Importantly, MSC transplantation improved cardiac function in these rats, as indicated by a significant decrease in LV end-diastolic pressure and an increase in LV dP/dt_{max}. Thus, the improvement in cardiac function may be a result of MSC-induced myocardial regeneration; however, further studies are necessary to investigate the mechanisms by which MSCs develop into cardiac myocyte–like cells.

Some of the transplanted MSCs were positive for a vascular endothelial cell marker and participated in vessel formation. MSC transplantation significantly increased capillary density in the myocardium. SMA staining revealed that MSCs differentiated into vascular smooth muscle cells, which play an important role in vessel maturation. Earlier studies have shown that transplantation of MNCs induces therapeutic angiogenesis in patients with limb ischemia or ischemic heart disease.[20–22] The angiogenic potential of MNCs is mediated at least in part by production by the cells of a variety of angiogenic factors.[24] Although MSCs have also been shown to produce VEGF,[10,25] there has been no study to compare their production between MSCs and MNCs. The present study demonstrated that MSCs secreted ≈4-fold more VEGF compared with MNCs. Furthermore, MSCs secreted large amounts of HGF and AM, potent angiogenic factors.[26–30] Taking these findings together, MSCs may contribute to neovascularization in the myocardium not only through their ability to generate capillary-like structures but also through growth factor–mediated paracrine regulation. Myocardial blood flow abnormalities have been documented in patients with heart failure caused by DCM.[12] Thus, it is possible that MSC-induced neovascularization contributes to improvement in cardiac function.

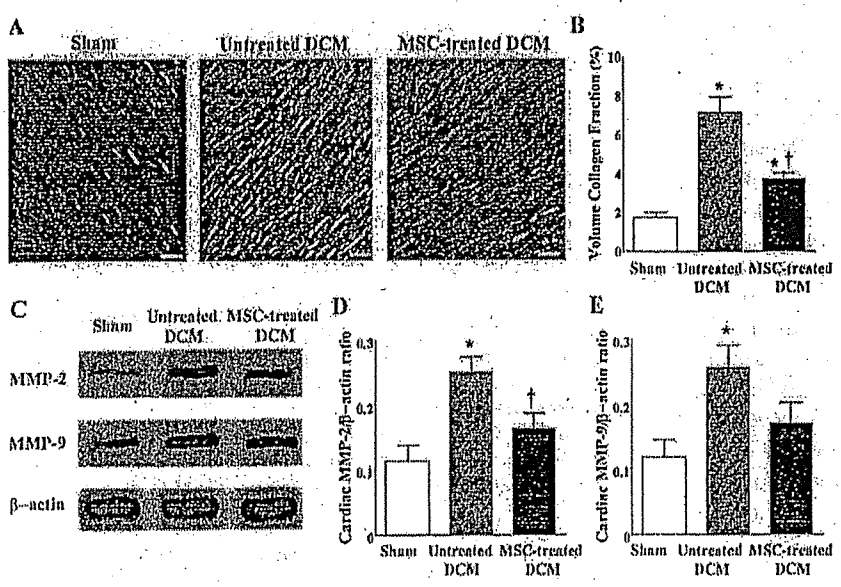

Figure 7. Effects of MSC transplantation on myocardial fibrosis. A, Photomicrographs show representative myocardial sections stained with Masson's trichrome. Scale bars=10 μm. B, Quantitative analysis demonstrated that the collagen volume fraction in the MSC-treated DCM group was significantly smaller than that in the untreated DCM group. C, Representative Western blots for MMPs-2 and -9 and β-actin in the heart. D and E, Quantitative analysis of cardiac tissue contents of MMP-2 and -9. Data are mean±SEM *P<0.05 vs sham group; †P<0.05 vs untreated DCM group.

HGF has not only angiogenic but also cardioprotective effects, including antiapoptotic, mitogenic, and antifibrotic activities.[26,27] *HGF* gene transfer into the myocardium improves myocardial function and geometry.[28] In particular, the antifibrotic effects of HGF through inhibition of transforming growth factor-β expression is beneficial for heart failure. Cultured MSCs secreted a large amount of HGF. In vivo, transplantation of MSCs slightly increased plasma HGF in rats. It significantly attenuated the development of myocardial fibrosis in a rat model of DCM. These results suggest that MSC-derived HGF may contribute to improvements in cardiac function partly through its antifibrotic effects.

MSCs also produced AM, a potent vasodilator and cardioprotective peptide.[29] We have shown that AM prevents cardiomyocyte apoptosis through the phosphatidylinositol 3-kinase/Akt–dependent pathway[16] and that it has potent angiogenic effects.[30] AM inhibits proliferation of cardiac fibroblasts through the cAMP-dependent pathway.[31] Administration of AM inhibits LV remodeling and improves cardiac function in heart failure.[32–34] In the present study, cultured MSCs secreted a large amount of AM in vitro. In vivo, transplantation of MSCs markedly increased plasma AM level. Taken together, these findings suggest that MSCs may exert their cardioprotective effects through AM-mediated paracrine regulation.

IGF-1, a growth hormone mediator, plays an important role in myocardial and skeletal muscle growth.[35,36] Administration of IGF-1 improves cardiac function after myocardial infarction through enhancement of myocardial growth.[37] Its protective and antiapoptotic properties have been demonstrated in different models of myocardial ischemia.[38] Furthermore, IGF-1 exerts Ca^{2+}-dependent, positive inotropic effects through a phosphatidylinositol 3-kinase–dependent pathway.[39] Interestingly, the present study demonstrated that MSCs secreted significant amounts of IGF-1 in vitro, 10-fold greater than MNCs. These findings raise the possibility that MSC-derived IGF-1 may participate in myocardial growth and enhancement of myocardial contractility in a rat model of DCM.

MMPs also play a crucial role in extracellular remodeling in heart failure.[40] In fact, pharmacological inhibition of MMP activities prevents progressive LV remodeling in an animal model of heart failure.[41] In the present study, cardiac MMP-2 and MMP-9 were increased in rats with DCM, which is consistent with recent findings in patients with heart failure.[40,42] Interestingly, MSC transplantation attenuated the increases in cardiac MMP-2 and MMP-9 in a rat model of DCM. Although the underlying mechanisms remain unclear, MSC transplantation may influence extracellular remodeling in heart failure.

The present study has some limitations. First, immunohistochemical evidence suggests differentiation of MSCs into cardiomyocytes, vascular endothelial cells, and smooth muscle cells. However, further studies are necessary to convincingly demonstrate differentiation of MSCs into a specific cell type. Second, the model of DCM used in this study was an injury model, and the effects of treatment may be related to attenuation of the injury rather than to the established cardiomyopathy. Nonetheless, the experiment was performed 5 to 9 weeks after myosin injection, by which time inflammatory changes were hardly observed and had been replaced by fibrosis.[43]

Conclusions

MSC transplantation improved cardiac function in a rat model of DCM, possibly through induction of myogenesis and angiogenesis, as well as by inhibition of myocardial fibrosis. The beneficial effects of MSCs may be mediated at least in part by their differentiation into cardiomyocytes and vascular cells and by their ability to supply large amounts of angiogenic, antiapoptotic, and mitogenic factors. Thus, MSC transplantation has potential as a new therapeutic strategy for the treatment of DCM.

Acknowledgments

This work was supported by research grants for cardiovascular disease (16C-6) and Human Genome Tissue Engineering 009 from the Ministry of Health, Labor and Welfare; the Industrial Technology Research Grant Program in '03 from the New Energy and Industrial Technology Development Organization of Japan; a research grant from the Japan Cardiovascular Research Foundation; and Promotion of Fundamental Studies in Health Science of the Organization for Pharmaceutical Safety and Research of Japan.

References

1. Cohn JN. The management of chronic heart failure. *N Engl J Med.* 1996;335:490–498.
2. Dec GW, Fuster V. Idiopathic dilated cardiomyopathy. *N Engl J Med.* 1994;331:1564–1575.
3. Beltrami AP, Urbanek K, Kajstura J, Yan SM, Finato N, Bussani R, Nadal-Ginard B, Silvestri F, Leri A, Beltrami CA, Anversa P. Evidence that human cardiac myocytes divide after myocardial infarction. *N Engl J Med.* 2001;344:1750–1757.
4. Pittenger MF, Mackay AM, Beck SC, Jaiswal RK, Douglas R, Mosca JD, Moorman MA, Simonetti DW, Craig S, Marshak DR. Multilineage potential of adult human mesenchymal stem cells. *Science.* 1999;284:143–147.
5. Reyes M, Dudek A, Jahagirdar B, Koodie L, Marker PH, Verfaillie CM. Origin of endothelial progenitors in human postnatal bone marrow. *J Clin Invest.* 2002;109:337–346.
6. Toma C, Pittenger MF, Cahill KS, Byrne BJ, Kessler PD. Human mesenchymal stem cells differentiate to a cardiomyocyte phenotype in the adult murine heart. *Circulation.* 2002;105:93–98.
7. Mangi AA, Noiseux N, Kong D, He H, Rezvani M, Ingwall JS, Dzau VJ. Mesenchymal stem cells modified with Akt prevent remodeling and restore performance of infarcted hearts. *Nat Med.* 2003;9:1195–1201.
8. Makino S, Fukuda K, Miyoshi S, Konishi F, Kodama H, Pan J, Sano M, Takahashi T, Hori S, Abe H, Hata J, Umezawa A, Ogawa S. Cardiomyocytes can be generated from marrow stromal cells in vitro. *J Clin Invest.* 1999;103:697–705.
9. Shake JG, Gruber PJ, Baumgartner WA, Senechal G, Meyers J, Redmond JM, Pittenger MF, Martin BJ. Mesenchymal stem cell implantation in a swine myocardial infarct model: engraftment and functional effects. *Ann Thorac Surg.* 2002;73:1919–1925.
10. Al-Khaldi A, Al-Sabti H, Galipeau J, Lachapelle K. Therapeutic angiogenesis using autologous bone marrow stromal cells: improved blood flow in a chronic limb ischemia model. *Ann Thorac Surg.* 2003;75:204–209.
11. Al-Khaldi A, Eliopoulos N, Martineau D, Lejeune L, Lachapelle K, Galipeau J. Postnatal bone marrow stromal cells elicit a potent VEGF-dependent neoangiogenic response in vivo. *Gene Ther.* 2003;10:621–629.
12. Parodi O, De Maria R, Oltrona L, Testa R, Sambuceti G, Roghi A, Merli M, Belingheri L, Accinni R, Spinelli F, Pellegrini A, Baroldi G. Myocardial blood flow distribution in patients with ischemic heart disease or dilated cardiomyopathy undergoing heart transplantation. *Circulation.* 1993;88:509–522.
13. Kodama M, Zhang S, Hanawa H, Saeki M, Inomata T, Suzuki K, Koyama S, Shibata A. Effects of 15-deoxyspergualin on experimental autoimmune giant cell myocarditis of the rat. *Circulation.* 1995;91:1116–1122.
14. Watanabe K, Ohta Y, Nakazawa M, Higuchi H, Hasegawa G, Naito M, Fuse K, Ito M, Hirono S, Tanabe N, Hanawa H, Kato K, Kodama M, Aizawa Y. Low dose carvedilol inhibits progression of heart failure in rats with dilated cardiomyopathy. *Br J Pharmacol.* 2000;130:1489–1495.

15. Nagaya N, Uematsu M, Kojima M, Ikeda Y, Yoshihara F, Shimizu W, Hosoda H, Hirota Y, Ishida H, Mori H, Kangawa K. Chronic administration of ghrelin improves left ventricular dysfunction and attenuates development of cardiac cachexia in rats with heart failure. *Circulation*. 2001;104:1430–1435.
16. Okumura H, Nagaya N, Itoh T, Okano I, Hino J, Mori K, Tsukamoto Y, Ishibashi-Ueda H, Miwa S, Tambara K, Toyokuni S, Yutani C, Kangawa K. Adrenomedullin infusion attenuates myocardial ischemia/reperfusion injury through the phosphatidylinositol 3-kinase/Akt-dependent pathway. *Circulation*. 2004;109:242–248.
17. Messina LM, Podrazik RM, Whitehill TA, Ekhterae D, Brothers TE, Wilson JM, Burkel WE, Stanley JC. Adhesion and incorporation of lacZ-transduced endothelial cells into the intact capillary wall in the rat. *Proc Natl Acad Sci U S A*. 1992;89:12018–12022.
18. Harada M, Itoh H, Nakagawa O, Ogawa Y, Miyamoto Y, Kuwahara K, Ogawa E, Igaki T, Yamashita J, Masuda I, Yoshimasa T, Tanaka I, Saito Y, Nakao K. Significance of ventricular myocytes and nonmyocytes interaction during cardiocyte hypertrophy: evidence for endothelin-1 as a paracrine hypertrophic factor from cardiac nonmyocytes. *Circulation*. 1997;96:3737–3744.
19. Ohta H, Tsuji T, Asai S, Sasakura K, Teraoka H, Kitamura K, Kangawa K. A simple immunoradiometric assay for measuring the entire molecules of adrenomedullin in human plasma. *Clin Chim Acta*. 1999;287:B131–B143.
20. Murohara T, Ikeda H, Duan J, Shintani S, Sasaki K, Eguchi H, Onitsuka I, Matsui K, Imaizumi T. Transplanted cord blood-derived endothelial precursor cells augment postnatal neovascularization. *J Clin Invest*. 2000;105:1527–1536.
21. Tateishi-Yuyama E, Matsubara H, Murohara T, Ikeda U, Shintani S, Masaki H, Amano K, Kishimoto Y, Yoshimoto K, Akashi H, Shimada K, Iwasaka T, Imaizumi T. Therapeutic Angiogenesis using Cell Transplantation (TACT) Study Investigators. Therapeutic angiogenesis for patients with limb ischaemia by autologous transplantation of bone-marrow cells: a pilot study and a randomised controlled trial. *Lancet*. 2002;360:427–435.
22. Tse HF, Kwong YL, Chan JK, Lo G, Ho CL, Lau CP. Angiogenesis in ischaemic myocardium by intramyocardial autologous bone marrow mononuclear cell implantation. *Lancet*. 2003;4:47–49.
23. Min JY, Sullivan MF, Yang Y, Zhang JP, Converso KL, Morgan JP, Xiao YF. Significant improvement of heart function by cotransplantation of human mesenchymal stem cells and fetal cardiomyocytes in postinfarcted pigs. *Ann Thorac Surg*. 2002;74:1568–1575.
24. Kamihata H, Matsubara H, Nishiue T, Fujiyama S, Tsutsumi Y, Ozono R, Masaki H, Mori Y, Iba O, Tateishi E, Kosaki A, Shintani S, Murohara T, Imaizumi T, Iwasaka T. Implantation of bone marrow mononuclear cells into ischemic myocardium enhances collateral perfusion and regional function via side supply of angioblasts, angiogenic ligands, and cytokines. *Circulation*. 2001;104:1046–1052.
25. Kinnaird T, Stabile E, Burnett MS, Lee CW, Barr S, Fuchs S, Epstein SE. Marrow-derived stromal cells express genes encoding a broad spectrum of arteriogenic cytokines and promote in vitro and in vivo arteriogenesis through paracrine mechanisms. *Circ Res*. 2004;94:678–685.
26. Nakamura T, Nishizawa T, Hagiya M, Seki T, Shimonishi M, Sugimura A, Tashiro K, Shimizu S. Molecular cloning and expression of human hepatocyte growth factor. *Nature*. 1989;342:440–443.
27. Nakamura T, Mizuno S, Matsumoto K, Sawa Y, Matsuda H, Nakamura T. Myocardial protection from ischemia/reperfusion injury by endogenous and exogenous HGF. *J Clin Invest*. 2000;106:1511–1519.
28. Li Y, Takemura G, Kosai K, Yuge K, Nagano S, Esaki M, Goto K, Takahashi T, Hayakawa K, Koda M, Kawase Y, Maruyama R, Okada H, Minatoguchi S, Mizuguchi H, Fujiwara T, Fujiwara H. Postinfarction treatment with an adenoviral vector expressing hepatocyte growth factor relieves chronic left ventricular remodeling and dysfunction in mice. *Circulation*. 2003;107:2499–2506.
29. Kitamura K, Kangawa K, Kawamoto M, Ichiki Y, Nakamura S, Matsuo H, Eto T. Adrenomedullin: a novel hypotensive peptide isolated from human pheochromocytoma. *Biochem Biophys Res Commun*. 1993;192:553–560.
30. Tokunaga N, Nagaya N, Shirai M, Tanaka E, Ishibashi-Ueda H, Harada-Shiba M, Kanda M, Ito T, Shimizu W, Tabata Y, Uematsu M, Nishigami K, Sano S, Kangawa K, Mori H. Adrenomedullin gene transfer induces therapeutic angiogenesis in a rabbit model of chronic hind limb ischemia: benefits of a novel nonviral vector, gelatin. *Circulation*. 2004;109:526–531.
31. Tsuruda T, Kato J, Kitamura K, Kawamoto M, Kuwasako K, Imamura T, Koiwaya Y, Tsuji T, Kangawa K, Eto T. An autocrine or a paracrine role of adrenomedullin in modulating cardiac fibroblast growth. *Cardiovasc Res*. 1999;43:958–967.
32. Nishikimi T, Yoshihara F, Horinaka S, Kobayashi N, Mori Y, Tadokoro K, Akimoto K, Minamino N, Kangawa K, Matsuoka H. Chronic administration of adrenomedullin attenuates transition from left ventricular hypertrophy to heart failure in rats. *Hypertension*. 2003;42:1034–1041.
33. Nakamura R, Kato J, Kitamura K, Onitsuka H, Imamura T, Cao Y, Marutsuka K, Asada Y, Kangawa K, Eto T. Adrenomedullin administration immediately after myocardial infarction ameliorates progression of heart failure in rats. *Circulation*. 2004;110:426–431.
34. Nagaya N, Satoh T, Nishikimi T, Uematsu M, Furuichi S, Sakamaki F, Oya H, Kyotani S, Nakanishi N, Goto Y, Masuda Y, Miyatake K, Kangawa K. Hemodynamic, renal, and hormonal effects of adrenomedullin infusion in patients with congestive heart failure. *Circulation*. 2000;101:498–503.
35. Fuller J, Mynett JR, Sugden PH. Stimulation of cardiac protein synthesis by insulin-like growth factors. *Biochem J*. 1992;282:85–90.
36. Florini JR, Ewton DZ, Coolican SA. Growth hormone and the insulin-like growth factor system in myogenesis. *Endocr Rev*. 1996;17:481–517.
37. Cittadini A, Stromer H, Katz SE, Clark R, Moses AC, Morgan JP, Douglas PS. Differential cardiac effects of growth hormone and insulin-like growth factor-1 in the rat: a combined in vivo and in vitro evaluation. *Circulation*. 1996;93:800–809.
38. Li Q, Li B, Wang X, Leri A, Jana KP, Liu Y, Kajstura J, Baserga R, Anversa P. Overexpression of insulin-like growth factor-1 in mice protects from myocyte death after infarction, attenuating ventricular dilation, wall stress, and cardiac hypertrophy. *J Clin Invest*. 1997;100:1991–1999.
39. von Lewinski D, Voss K, Hulsmann S, Kogler H, Pieske B. Insulin-like growth factor-1 exerts Ca^{2+}-dependent positive inotropic effects in failing human myocardium. *Circ Res*. 2003;92:169–176.
40. Thomas CV, Coker ML, Zellner JL, Handy JR, Crumbley AJ 3rd, Spinale FG. Increased matrix metalloproteinase activity and selective upregulation in LV myocardium from patients with end-stage dilated cardiomyopathy. *Circulation*. 1998;97:1708–1715.
41. Spinale FG, Coker ML, Krombach SR, Mukherjee R, Hallak H, Houck WV, Clair MJ, Kribbs SB, Johnson LL, Peterson JT, Zile MR. Matrix metalloproteinase inhibition during the development of congestive heart failure: effects on left ventricular dimensions and function. *Circ Res*. 1999;85:364–376.
42. Spinale FG, Coker ML, Heung LJ, Bond BR, Gunasinghe HR, Etoh T, Goldberg AT, Zellner JL, Crumbley AJ. A matrix metalloproteinase induction/activation system exists in the human left ventricular myocardium and is upregulated in heart failure. *Circulation*. 2000;102:1944–1949.
43. Kodama M, Matsumoto Y, Fujiwara M, Zhang SS, Hanawa H, Itoh E, Tsuda T, Izumi T, Shibata A. Characteristics of giant cells and factors related to the formation of giant cells in myocarditis. *Circ Res*. 1991;69:1042–1050.

CLINICAL PERSPECTIVE

Transplantation of stem or progenitor cells has the potential to improve and restore cardiac function. To date, experimenters investigating the possible therapeutic effects of stem cells in the heart have used models of infarction, and little information is available about the therapeutic potential of cell transplantation for heart failure due to dilated cardiomyopathy. In the present study, we demonstrated that transplantation of stem cells improved cardiac function in a model of myocarditis. We found evidence that stem cells may work to improve heart function by both myogenesis and angiogenesis while inhibiting myocardial fibrosis. Based on our data, part of the mechanism for this improvement may occur through the action of stem cells as a source of growth factors and cytokines in the heart. This study supports the overall notion that mesenchymal stem cells transplanted into the failing heart have potential as a new therapeutic strategy for the treatment of dilated cardiomyopathy.

Prognostic Usefulness of Serum Uric Acid After Acute Myocardial Infarction (The Japanese Acute Coronary Syndrome Study)

Sunao Kojima, MD[a,*], Tomohiro Sakamoto, MD[a], Masaharu Ishihara, MD[b], Kazuo Kimura, MD[c], Shunichi Miyazaki, MD[d], Masakazu Yamagishi, MD[d], Chuwa Tei, MD[e], Hisatoyo Hiraoka, MD[f], Masahiro Sonoda, MD[g], Kazufumi Tsuchihashi, MD[h], Nobuo Shimoyama, MD[i], Takashi Honda, MD[j], Yasuhiro Ogata, MD[k], Kunihiko Matsui, MD[l], and Hisao Ogawa, MD[a], on behalf of the Japanese Acute Coronary Syndrome Study (JACSS) Investigators*

Serum uric acid (UA) levels reflect circulating xanthine oxidase activity and oxidative stress production. Hyperuricemia has been identified in patients who have congestive heart failure and is a marker of poor prognosis in such patients. We investigated the relation between serum UA levels and Killip's classification suggestive of the severity of heart failure and whether hyperuricemia influences mortality of patients who have acute myocardial infarction (AMI). Using the Japanese Acute Coronary Syndrome Study database, we evaluated 1,124 consecutive patients who were hospitalized within 48 hours of onset of symptoms of AMI from January to December 2002. There was a close relation between serum UA concentration and Killip's classification. Patients who developed short-term adverse events had high UA concentrations. Serum UA levels, Killip's class, age, and peak creatine phosphokinase level were significant predictors of long-term mortality. The hazard ratio for patients in the highest quartile of UA was 3.7 compared with those in the lowest quartile for death after AMI after adjustment for independent factors that were related to mortality. The combination of the best UA cutoff (447 μmol/L) for predicting survival based on receiver-operating characteristics analysis and Killip's class significantly predicted the prognosis of acute and long-term AMI-related complications. In conclusion, our results suggest that hyperuricemia after AMI is associated with the development of heart failure. Serum UA level is a suitable marker for predicting AMI-related future adverse events, and the combination of Killip's class and serum UA level after AMI is a good predictor of mortality in patients who have AMI. © 2005 Elsevier Inc. All rights reserved. **(Am J Cardiol 2005;96:489–495)**

Previous studies have reported that a high concentration of uric acid (UA) is a strong marker of an unfavorable prognosis of moderate to severe heart failure and cardiovascular disease.[1,2] Therefore, we hypothesized that serum UA concentrations would correlate with Killip's classification suggestive of the severity of left ventricular failure and that hyperuricemia was related to mortality in patients who had acute myocardial infarction (AMI).

Methods

Data sources: The Japanese Acute Coronary Syndrome Study (JACSS) is a retrospective and multicenter observational study that is being conducted at 35 medical institutions in Japan. The JACSS database includes information on 1,124 consecutive patients who were hospitalized at participating institutions within 48 hours after onset of symptoms of AMI from January to December 2002 and whose UA

The [a]Department of Cardiovascular Medicine, Graduate School of Medical Sciences, Kumamoto University, Kumamoto; the [b]Department of Cardiology, Hiroshima City Hospital, Hiroshima; the [c]Division of Cardiology, Yokohama City University Medical Center, Yokohama; the [d]Division of Cardiology, Department of Internal Medicine, National Cardiovascular Center, Suita; the [e]Department of Cardiovascular Respiratory and Metabolic Medicine, Graduate School of Medicine, Kagoshima University, Kagoshima; the [f]Department of Internal Medicine and Molecular Science, Graduate School of Medicine, Osaka University, Suita; the [g]Second Department of Cardiology, National Hospital Kyushu Cardiovascular Center, Kagoshima; the [h]Second Department of Internal Medicine, Sapporo Medical University School of Medicine, Sapporo; the [i]Division of Cardiology, Oita National Hospital, Oita; and the [j]Cardiovascular Center, Saiseikai Kumamoto Hospital, the [k]Department of Cardiology, Japanese Red Cross Kumamoto Hospital, and the [l]Department of General Medicine, Kumamoto University Hospital, Kumamoto City, Japan. Manuscript received January 18, 2005; revised manuscript received and accepted March 30, 2005.

This study was supported by research grants for cardiovascular disease (14C-1 and 14C-4) from the Ministry of Health, Labour and Welfare, Tokyo, Japan.

* Corresponding author. Tel.: 81-96-373-5175; fax: 81-96-362-3256.
E-mail address: kojimas@kumamoto-u.ac.jp (S. Kojima).

0002-9149/05/$ – see front matter © 2005 Elsevier Inc. All rights reserved.
doi:10.1016/j.amjcard.2005.04.007

concentrations were measured on admission. AMI was defined as increased myocardial enzyme concentrations with typical chest pain persisting >30 minutes or electrocardiographic changes (including ischemic ST-segment depression, ST-segment elevation, or pathologic Q waves). Increased enzyme concentrations were defined as peak creatine phosphokinase levels >2 times the upper limit of normal. The study protocol was reviewed and approved by the ethical committee of each participating institution.

Patients: Patients who were treated with antihypertensive drugs or those whose baseline blood pressure was ≥140/90 mm Hg were considered to have hypertension. Diabetes mellitus was diagnosed according to criteria of the World Health Organization.[3] Hyperlipidemia was defined as a total cholesterol level ≥220 mg/dl and/or a triglyceride level ≥150 mg/dl. Cigarette smoking was defined as active smoking.

Serum UA concentrations and other laboratory data: Blood samples for measurements of serum UA concentrations and other biochemical assessments were obtained intravenously immediately after admission. UA and other biochemical variables were measured according to standard techniques adopted by the participating institutions, and serum creatinine and UA concentrations were expressed as micromoles per liter. UA was treated as a continuous variable and as a categorical variable, and variables were divided into quartiles according to serum UA concentrations.

Coronary angiography and reperfusion therapy: Allocation of coronary angiography and reperfusion therapy was determined by physicians. The perfusion grade of the infarct-related artery was assessed according to the Thrombolysis in Myocardial Infarction (TIMI) study classification.[4] The final TIMI flow grade was assessed on the final shot of emergency coronary angiography.

Short- and long-term morbidities and mortalities: The primary end point was mortality from any cause. Major adverse cardiac events, including cardiac death, reinfarction, unstable angina, heart failure, and stroke, were also assessed. We evaluated 30-day adverse events and mortality rates after AMI during long-term follow-up.

Statistical analysis: Subjects in the analysis were categorized into 4 quartiles according to their serum UA levels. Differences in frequencies were analyzed by the chi-square method. Continuous data were compared by 1-way analysis of variance followed by Scheffé's F test. Clinical characteristics considered to be associated with serum UA concentrations were included in the models. These characteristics included age, gender, background illness (hypertension, diabetes mellitus, or hyperlipidemia), smoking, admission characteristics (body mass index, serum creatinine levels, previous myocardial infarction, premedication, and preinfarction angina pectoris), time from symptom onset, coronary angiographic findings (multivessel involvement, culprit location, occlusion of the infarct-related coronary artery, and final TIMI flow grade in the acute phase), peak creatine phosphokinase levels, and left ventricular ejection fraction during the AMI and at follow-up. Killip's classes on hospital admission, depending on clinical manifestations of heart failure, were also assessed (class I = no heart failure; class II = S_3 and/or basal lung crepitations; class III = acute pulmonary edema; class IV = cardiac shock).[5]

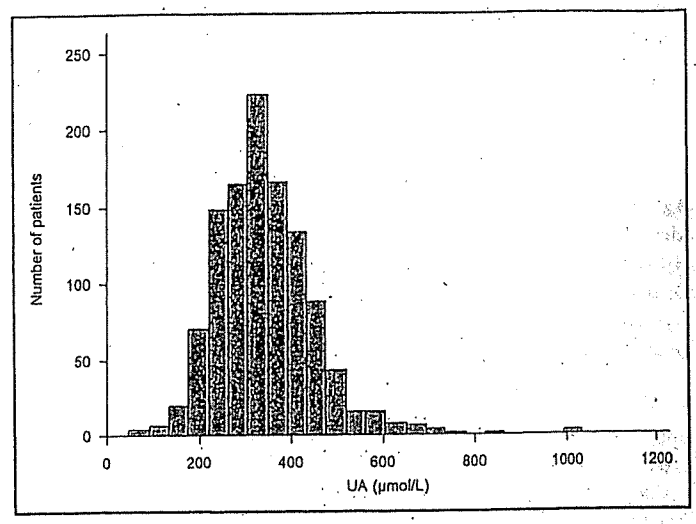

Figure 1. Histogram of distribution of baseline serum UA concentrations in 1,124 study patients.

Odds ratios and 95% confidence intervals of 30-day adverse events and long-term mortality were calculated using logistic regression analysis. Cox's proportional hazards analysis was performed to assess risk of mortality. Cumulative event curves were plotted using the Kaplan-Meier survival method and differences between curves were tested for statistical significance by the log-rank analysis. We performed multivariate analysis as the need arose (StatView 5.0, Abacus Concept, Inc., Berkeley, California). A p value <0.05 was considered statistically significant in all analyses. All data were expressed as mean ± SD unless otherwise indicated.

To compare different predictive values at a particular time point, areas under the curve for sensitivity and specificity were constructed. The best prognostic cutoff for predicting mortality at the respective times was defined as that which yielded the highest product of sensitivity and specificity.[6] To contrast prognostic accuracy, a receiver-operating characteristic curve was generated using LABROC5 (http://www.radiology.vehicago.edu/k-l/roc_soft.htm), which was provided by Metz et al.[7]

Results

Patients' clinical background and angiographic demographics: Figure 1 shows the distribution of serum UA levels. Serum UA concentrations ranged from 48 to 1,035 μmol/L (0.8 to 17.4 mg/dl). The median UA concentration was 333 μmol/L (5.6 mg/dl) and the interquartile interval was 274 to 399 μmol/L (4.6 to 6.7 mg/dl). Coronary reper-

Table 1
Clinical and angiographic characteristics of patients with acute myocardial infarction by quartiles of serum uric acid concentration

Variables	UA Quartile (μmol/L)			
	1 (<274) (n = 273)	2 (274–333) (n = 299)	3 (333–399) (n = 276)	4 (>399) (n = 276)
Age (yrs)	69 ± 11	67 ± 13	67 ± 12	68 ± 13
Men	55%	75%*	78%*	76%*
Hypertension	52%	52%	58%	65%*†
Diabetes mellitus	34%	29%	29%	33%
Hyperlipidemia	32%	35%	39%	38%
Body mass index (kg/m^2)	22.8 ± 3.3	23.8 ± 3.3*	23.8 ± 3.1*	24.2 ± 3.4*
Current smoker	38%	51%*	55%*	43%‡
Serum creatinine (μmol/L)	65.0 ± 29.2	80.5 ± 84.6	94.4 ± 104.5*	112.7 ± 85.9*†
Previous myocardial infarction	7%	11%	13%*	17%*†
Premedication				
Antiplatelet use	12%	14%	17%	18%
Statin use	8%	11%	9%	7%
Angiotensin-1 receptor blocker use	3%	5%	7%	7%
Preinfarction angina pectoris	37%	40%	34%	31%
Time from symptom onset (h)	6.5 ± 8.3	6.8 ± 9.3	5.5 ± 7.1	6.2 ± 8.8
Killip's class III–IV	5%	6%	11%*	24%*†‡
Peak creatine phosphokinase (IU/L)	2,577 ± 2,032	3,088 ± 2,995	3,056 ± 2,709	3,643 ± 4,876*
Coronary multivessel involvement	42%	46%	45%	45%
Culprit LAD location	47%	40%	42%	42%
Occlusion of IRCA on acute phase	62%	61%	59%	61%
Final TIMI grade 3 flow	89%	88%	86%	87%
Left ventricular ejection fraction				
Acute phase (n = 360)	51 ± 13%	53 ± 9%	49 ± 12%	48 ± 13%†
Discharge (n = 539)	55 ± 12%	53 ± 11%	52 ± 14%	54 ± 12%

* $p < 0.05$ versus quartile 1; † $p < 0.05$ versus quartile 2; ‡ $p < 0.05$ versus quartile 3, by chi-square test between quartiles or 1-way analysis of variance followed by Scheffé's F test.
IRCA = infarct-related coronary artery; LAD = left anterior descending.

fusion therapy was performed in 943 patients (84%) immediately after admission: coronary stent implantation in 743 patients (66%), conventional balloon angioplasty in 146 patients (13%), and intracoronary thrombolysis or intravenous thrombolysis in 54 patients (5%). Patients were followed for an average period of 454 ± 159 days (maximum 699).

Greater proportions of men, smokers, and those who had previous myocardial infarction were seen in the higher UA quartiles. In addition, there was a graded relation between increasing body mass index and creatinine and higher UA quartiles. High Killip's class and high peak levels of creatine phosphokinase were also observed in the high UA quartile (Table 1).

Table 2
Multiple regression analysis for serum uric acid levels on admission

Independent Variables	Regression Coefficients	SE	95% CI	p Value
Men	0.602	0.119	0.369–0.835	<0.0001
Body mass index	0.089	0.016	0.058–0.121	<0.0001
Killip's classification	0.293	0.066	0.165–0.422	<0.0001
Serum creatinine	0.377	0.058	0.263–0.492	<0.0001
Previous myocardial infarction	0.520	0.160	0.207–0.833	0.0012
Hypertension	0.301	0.108	0.090–0.513	0.0052

The p values reflect multiple regression analysis after stepwise regression, including all variables listed in Table 1.
CI = confidence interval.

Clinical determinants of serum UA concentrations: To assess determinants of serum UA concentrations, multiple regression analysis was performed after a stepwise regression that included all clinical variables listed in Table 1. Results showed that serum UA concentrations were significantly correlated with male gender, body mass index, Killip's class, serum creatinine, previous myocardial infarction, and hypertension ($r = 0.3659$, $p < 0.0001$; Table 2).

Short-term adverse events and long-term mortality: Patients who developed short-term adverse events had high UA concentrations. Patients in quartile 4 were >5 times more likely to show a 30-day all-cause mortality compared with those in quartile 1 (Table 3). Multivariate analysis that included all variables that were significantly associated with all-cause mortality in univariate analysis showed that UA concentrations, in addition to Killip's class, age, and peak creatine phosphokinase, closely correlated with all-cause mortality (Table 4). Figure 2 shows survival without all-cause mortality in patients after AMI based on UA quartiles. The hazard ratio for patients in quartile 4 was 3.7 compared with that of patients in quartile 1 for death after AMI after nonadjustment and adjustment for independent factors that were closely associated with all-cause mortality (Table 5).

Table 3
Thirty-day adverse events by quartiles of serum uric acid concentrations

UA Quartile (μmol/L)	30-Day Cardiac Death				30-Day MACE				30-Day Total Death			
		OR	95% CI	p Value		OR	95% CI	p Value		OR	95% CI	p Value
1 (<274; n = 273)	5 (2%)	1.000	—	—	15 (5%)	1.000	—	—	6 (2%)	1.000	—	—
2 (274–333; n = 299)	7 (2%)	1.285	0.403–4.097	0.6727	15 (5%)	0.908	0.435–1.895	0.7980	10 (3%)	1.540	0.552–4.295	0.4095
3 (333–399; n = 276)	8 (3%)	1.600	0.517–4.954	0.4150	15 (5%)	0.989	0.473–2.064	0.9754	8 (3%)	1.328	0.455–3.881	0.6037
4 (>399; n = 276)	30 (11%)	6.537	2.496–17.115	0.0001	39 (14%)	2.830	1.521–5.267	0.0010	31 (11%)	5.631	2.309–13.729	0.0001

OR values are based on logistic regression analysis regarding 30-day adverse events (cardiac death, MACE, and total death).
MACE = major adverse cardiac events; OR = odds ratio; other abbreviation as in Table 2.

Best UA cut-off concentration, Killip's classes, and long-term mortality: Receiver-operating characteristic areas under the curve (mean ± SEM) at 30 days, 6 months, and 1 year were 0.7072 ± 0.0455 (95% confidence interval 0.6125 to 0.7896), 0.7173 ± 0.0401 (95% confidence interval 0.6339 to 0.7902), and 0.7014 ± 0.0370 (95% confidence interval 0.6252 to 0.7695), respectively, and the receiver-operating characteristic area under the curve at 6 months was the largest. The sensitivity and specificity for prediction of mortality using the best cut-off value for serum UA levels at 6 months (447 μmol/L, 7.5 mg/dl) were 64% and 66%, respectively. Killip's classification and serum UA concentrations independently and significantly predicted poor prognosis; therefore, application of the best UA cut-off value to Killip's classes that were divided into 2 groups (low = Killip's classes I and II; high = Killip's classes III and IV) improved the positive and negative discriminatory powers for survival prediction (Figure 3). The hazard ratio of patients who were in a high Killip's class and had a serum UA concentration >447 μmol/L was ~22 compared with those who were in a low Killip's class and had a serum UA level ≤447 μmol/L for death after AMI, after adjusting for age and peak creatine phosphokinase level, which were closely associated with all-cause mortality (Table 6).

In patients who were in a high Killip's class and had a serum UA concentration ≥447 μmol/L (n = 57), TIMI grade 3 flow was associated with better 30-day and long-term survival rates compared with TIMI perfusion grade 0, 1, and 2 flows, although it was statistically insignificant (70% vs 55%, p = 0.2490, and 65% vs 45%, p = 0.1471, respectively).

Discussion

In the present study, we found a close relation between serum UA concentrations and Killip's classification suggestive of left ventricular failure. High UA concentrations on admission were strongly associated with adverse clinical outcome in patients who had AMI. The total mortality rate of patients whose serum UA concentrations were in the highest quartile was ~3.7 times higher than that in those whose UA concentrations were in the lowest quartile. Further, adding Killip's class to serum UA concentration improved its prognostic power.

Epidemiologic studies have suggested that hyperuricemia is a risk factor for cardiovascular disease.[8,9] Our results showed that serum UA concentrations correlate significantly with male gender, body mass index, serum creatinine concentrations, and hypertension. These results are similar to those of previous studies.[10,11] We also demonstrated that serum UA concentrations are influenced by Killip's classi-

Table 4
Predictors of mortality

Variable	Univariate Analysis			Multivariate Analysis		
	OR	95% CI	p Value	OR	95% CI	p Value
Killip's classification	2.608	2.173–3.131	<0.0001	2.125	1.711–2.639	<0.0001
Age (per yr)	1.067	1.042–1.092	<0.0001	1.059	1.029–1.090	<0.0001
Uric acid (per μmol/L)	1.005	1.003–1.006	<0.0001	1.004	1.002–1.006	<0.0001
Peak creatine phosphokinase (per IU/L)	1.000	1.000–1.000	<0.0001	1.000	1.000–1.000	0.0001
Serum creatinine (per μmol/L)	1.002	1.001–1.004	0.0004	—	—	—
Body mass index (per kg/m^2)	0.841	0.762–0.928	0.0006	—	—	—
Coronary vessel involvement	1.697	1.228–2.345	0.0014	—	—	—
Previous myocardial infarction	2.415	1.375–4.255	0.0022	—	—	—
Hyperlipidemia	2.550	1.363–4.771	0.0034	—	—	—
Final TIMI flow grade	0.738	0.549–0.994	0.0454	—	—	—

The p values in multivariate analysis as results of Cox's proportional hazards analysis after stepwise regression analysis including all variables that were significantly associated with all-cause mortality in univariate analysis.
Abbreviations as in Tables 2 and 3.

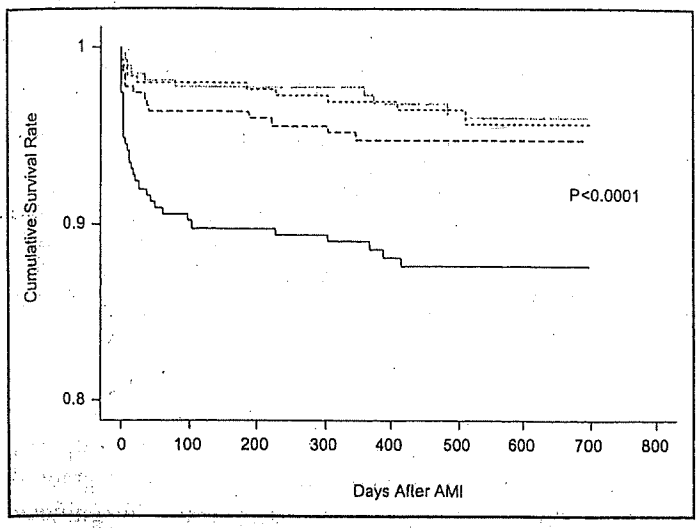

Figure 2. Survival without all-cause mortality in patients after AMI based on serum UA concentrations of <274 μmol/L in quartile 1 *(thin solid line)*, 274 to 333 μmol/L in quartile 2 *(short-dash line)*, 333 to 399 μmol/L in quartile 3 *(long-dash line)*, and >399 μmol/L in quartile 4 *(thick solid line)*.

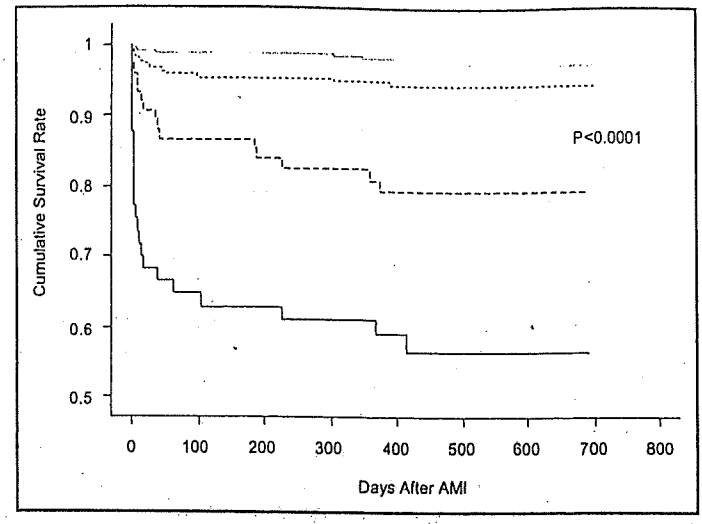

Figure 3. Survival without all-cause mortality in patients after AMI based on combinations of the best UA cut-off concentration of 447 μmol/L (7.5 mg/dl) for predicting survival and Killip's class: Killip's classes I and II plus a UA concentration ≤447 μmol/L *(thin solid line)*, Killip's classes I and II plus a UA concentration >447 μmol/L *(short-dash line)*, Killip's classes III and IV plus a UA concentration ≤447 μmol/L *(long-dash line)*, and Killip's classes III and IV plus a UA concentration >447 μmol/L *(thick solid line)*.

fication and previous myocardial infarction, which are considered to be deeply involved in decreased cardiac output that is caused by AMI.

Prompt restoration of myocardial blood flow is the therapeutic goal in AMI because early reperfusion decreases mortality rates.[12] In patients who had AMI, were in a high Killip's class, and had high UA concentrations, our results associated TIMI grade 3 flow with decreased short- and long-term mortality rates compared with TIMI perfusion grade 0, 1, and 2 flows; however, these differences were not significant in the present study. A failing heart due to AMI may cause tissue hypoperfusion and hypoxia, which trigger xanthine oxidase activation and oxidative stress production.[13,14] Xanthine oxidase and oxidative stress as reflected by UA may form a vicious cycle that promotes severe heart failure.[13,15] Therefore, UA may not be only a bystander marker but also a causative marker of mortality in patients who have AMI. In this regard, improvement of coronary reperfusion alone may be less effective in ameliorating heart failure and decreasing mortality rate in patients who have AMI and high UA level and are in a high Killip's class.

Adjunctive therapy designed to decrease xanthine oxidase activity and inhibit oxidative stress production is expected to sever the vicious cycle. The Losartan Intervention For Endpoint reduction in hypertension (LIFE) study demonstrated that lowering serum UA concentrations by losartan was associated with a beneficial effect on cardiovascular outcome.[16] The UA-lowering effect of atorvastatin may have contributed to the decrease in cardiovascular mortality in the Greek Atorvastatin and Coronary Heart Disease Evaluation (GREACE) study.[17] Therefore, any drug interventions, such as therapy to decrease serum UA level in addition to coronary reperfusion, may have a favorable effect on mortality in patients who have AMI.

Our study is limited by being a retrospective study. However, it included all patients who had AMI and were entered in the 2002 database. All patients were followed after onset of AMI, so that the results of the present study should reflect the actual condition of patients in Japan who have AMI.

Table 5
Association between uric acid quartiles and all-cause mortality

UA Quartile (μmol/L)	Total Death	Unadjusted			Adjusted		
		OR	95% CI	p Value	OR	95% CI	p Value
1 (<274; n = 273)	9 (3%)	1.000	—	—	1.000	—	—
2 (274–333; n = 299)	11 (4%)	1.098	0.455–2.650	0.8351	1.618	0.541–4.836	0.3892
3 (333–399; n = 276)	14 (5%)	1.542	0.668–3.564	0.3105	1.503	0.511–4.425	0.4594
4 (>399; n = 276)	33 (12%)	3.753	1.795–7.843	0.0004	3.716	1.417–9.741	0.00765

Hazard ratios compared with quartile 1 with regard to long-term mortality after nonadjustment and adjustment for independent factors that were closely associated with all-cause mortality in multivariate analysis (Killip's classification, age, and peak creatine phosphokinase level).

Abbreviations as in Tables 2 and 3.